Report on the first year's performance of HF radars in sea surface currents measurements

Technical report N: 05

Version 1.01

Authors: L. Quirós-Collazos, C. González-Haro, E. García-Ladona, J. Martínez, C. Bueno-Herrero, J. Isern-Fontanet

File: ICATMAR_SO_2025_05_1year_report_HFR_currents_v1.pdf

Date: August 13, 2025

Co-funded by the European Union
Generalitat de Catalunya
CSIC Consejo Superior de Investigaciones Científicas
Institut de Ciències del Mar

Abstract

This public ICATMAR report presents the analysis of operational data products derived from the first operating year of the ICATMAR High-Frequency Radar (HFR) network. The report is divided in three sections. The first one presents a description of the technical characteristics of the ICATMAR HFR network and the data period analysed here. The second one presents de description of the Quality Control (QC) model applied on the level 2 (L2) products, which correspond to radial velocity measures. Then, the performance of the L2 QC model on the 1^{st} year of available data is analysed, together with a general statistical assessment of radial velocity measures that passed the QC. Last section presents de description of the QC model applied on the level 3 (L3) products, which correspond to total velocity measures derived from the combination of radial velocities measured by each HFR. As in the previous section, the performance of the L3 QC model on the 1^{st} year of available data is analysed, together with a general statistical assessment of total velocity measures that passed the QC. Final part of this section includes the first exercise of ICATMAR HFR-derived data validation through the comparison with marine current measures from a Puertos del Estado fixed buoy and with Lagrangian trajectories of drifting objects.

How to cite:

Quirós-Collazos L., González-Haro C., García-Ladona E., Martínez J., Bueno-Herrero C., Isern-Fontanet J., 2025. *Report on the first year's performance of HF radars in sea surface currents measurements.* Technical report, n^{o}5, pp: 64. https://doi.org/10.20350/digitalCSIC/17509.

Contents

Control of Versions

Date	Changes	Name
22/11/2024	Initial version of the report.	LQC
30/05/2025	Addition of information to Sections 1 and 2.	CBH, LQC
30/07/2025	Main text corrections. Format corrections.	CGH
28/07/2025	Main text corrections. Format corrections. Updates on the `icatmar.sty` .	EGL
01/08/2025	Modifications on discussion of Section 4.4.	EGL, JM, LQC
05/08/2025	Final reviews	LQC

LQC = L. Quirós-Collazos
CGH = C. González-Haro
EGL = E. García-Ladona
JM = J. Martínez
CBH = C. Bueno-Herrero

List of Acronyms

APM	*Antenna Pattern Measurement*
CMEMS	*Copernicus Marine Environment Monitoring Service*
CSIC	*Consejo Superior de Investigaciones Científicas*
CTF	*CODAR Tabular Format*
EKE	*Eddy Kinetic Energy*
GDOP	*Geometrical Dilution Of Precision*
HFR	*High Frequency Radar*
ICATMAR	*Institut Català per a la Governança del Mar*
ICM	*Institut de Ciències del Mar*
JERICO	*Joint European Research Infrastructure network for Coastal Observatory*
L	*Level*
MUSIC	*Multiple Signal Classification*
PDF	*Probability Density Function*
QC	*Quality Control*
SAR	*Search And Rescue*
SOCIB	*Sistema de Observación y Predicción Costero de las Illes Balears*
UNESCO/IOC	*UNESCO Intergovernmental Oceanographic Commission*
US-IOOS	*United States Integrated Ocean Observing System*
UTC	*Universal Time Coordinated*

1 Introduction

The Catalan Institute of Research for the Governance of the Sea (ICATMAR) is a cooperation organization between the Government of Catalonia and the Spanish National Research Council (CSIC) through the Institute of Marine Sciences (ICM). It was officially created in December 2023 (BOE-A-2023-25106) with the aim to provide reliable and qualitative scientific products that serve administrations and society for the sustainable management of the marine environment and resources. Currently, ICATMAR consists of two services, the fishing advice service and the operational oceanography service. The purpose of the later is to provide near-real time monitoring data of the sea state and also the development of a forecast system for the short-term sea state evolution.

The infrastructure of the sea state monitoring system consists in a network of high frequency radars, a network of fixed mete-oceanic buoys and several types of drifting buoys. In particular, the deployment of the HFR antenna's array started in December 2022 with the installation of the first station at Cap de Creus (named CREU), followed by a second station installed at Cap sa Sal (named BEGU) in February 2023. This infrastructure measures sea surface currents in near-real time. The ICATMAR HFR network will be the third and the most extensive one of the North-West Mediterranean region, which is added to previously existing similar infrastructures: that from Puertos del Estado, which provides measures from the Ebre Delta area (in operation since 2014), and that from the SOCIB, that monitors the Eivissa Channel area (in operation since 2012) (Figure 1).

The aim of the present report is to evaluate the data obtained during the first year of operation of the ICATMAR HFR network. The report is structured in three main sections. Section 2 presents a general description of the current status of the ICATMAR HFR network, and sections 3 and 4 present the analysis of the the data quality and data itself of measures obtained during the first year of operation after the installation of the first two antennas, which are located in the northern sector of the Catalan coast (stations CREU and BEGU, see Figures 1 and 2). The data time-series analysed here comprises the period between 01/May/2023 00:00h and 30/April/2024 23:00h (both included).

More specifically, section 3 includes the description of the quality control (QC) model applied to radial velocity data (section 3.1), together with the performance of each of the QC tests over the analysed period (section 3.2). Based only on good quality radial data, the first four statistical moments and probability density functions (PDFs) have been estimated (section 3.3).

Section 4 includes the description of the QC model applied to total velocity data (section 4.1), together with the performance of each of the tests over the analysed period (section 4.2). Based only on good quality total velocity data, the first four statistical moments and PDFs have been estimated (section 4.3). Lastly, in section 4.4 the first validation exercise of the ICATMAR HFR derived data is presented by comparing with current measures derived from buoy of Begur from Puertos del Estado network and with Lagrangian trajectories of drifting objects.

The results obtained in this report will serve for refining the parameters of the QC models used for an HFR network operating in the oceanographic context of the Catalan sea, and also to get an overview of the average sea surface currents of this marine region.

2 The ICATMAR HFR network

The HFR network consists of seven antennas strategically distributed from north to south along the Catalan coast: Cap de Creus, Cap sa Sal, Cap de Tossa, Arenys de Mar Port, Barcelona Port, Ginesta Port, and Segur de Calafell Port (Figure 1, Table 1). This last antenna will enable a connection with the HFR network of the RIADE project, managed by Puertos del Estado. The RIADE project comprises three HFR stations located at Cap de Salou, Alfacada, and Port of Vinaròs, covering an area of 8,283 km^2.

Each HFR antenna provides measures of the sea surface current component projected on the direction towards the antenna in a radial coverage display. By combining these radial coverages, 2D surface current maps are generated with a spatial resolution of 3 km and an offshore coverage between 60 and 80 km, that gives a total coverage of 21,085 km^2 (Figure 1). These 2D maps contain information on the current velocity and direction of the first meter of sea surface.

2. THE ICATMAR HFR NETWORK

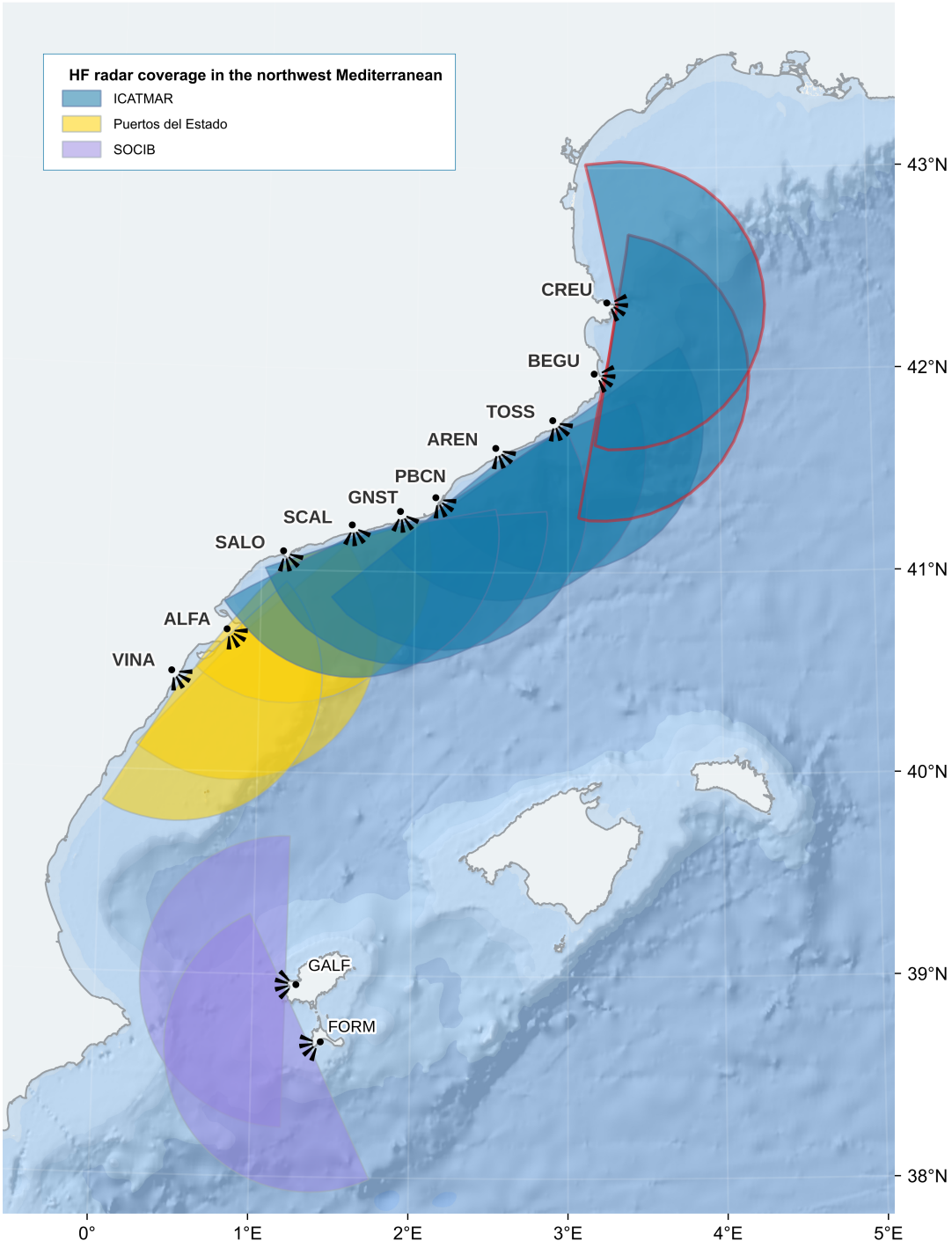

Figure 1: Distribution of the stations from the ICATMAR HFR network along the Catalan coast (see also Table 1). They are shown within the context of the NW Mediterranean region where the already existing networks of Puertos del Estado and SOCIB are also shown. Shaded areas indicate the theoretical observation area covered by each antenna; coverage areas highlighted in red correspond to CREU and BEGU stations, whose data time-series have been analysed in this report.

(a) (b)

Figure 2: HFR stations denoted as (a) CREU and (b) BEGU, which were installed in Cap de Creus and Cap sa Sal, respectively, during the first deployment phase of the ICATMAR HFR network.

2.1 Deployment chronology

The seven HFR antennas of the ICATMAR network have been deployed in three phases (Table 1, Figure 1). First phase took place between December 2022 and February 2023, when the two northern most antennas, named CREU and BEGU stations, were installed (Figure 2). Second phase took place between January and March 2024 with the installation of three antennas in the middle region of the Catalan coast, named as AREN, PBCN and GNST. Lastly, third installation phase took place between December 2024 and January 2025, when TOSS and SCAL stations were installed (see Table 1). The installation of TOSS station, allowed the connection between northern and central areas of the Catalan coast already covered by the ICATMAR HFR network, and with the installation of SCAL, areas covered by the ICATMAR and Puertos del Estado networks become connected, thus fully covering the whole Catalan coast (Figure 1). The completed infrastructure of the ICATMAR HFR network is making possible the near-real time monitoring of sea surface currents along the whole Catalan coast.

Station name	Location	Coordinates	Deployment date
CREU	Cap de Creus	42.32°N 3.32°E	December 2022
BEGU	Cap sa Sal	41.97°N 3.23°E	February 2023
TOSS	Cap de Tossa	41.72°N 2.93°E	December 2024
AREN	Port d'Arenys de Mar	41.58°N 2.56°E	December 2023
PBCN	Port de Barcelona	41.34°N 2.17°E	December 2023
GNST	Port Ginesta	41.26°N 1.92°E	December 2023
SCAL	Port Segur-Calafell	41.19°N 1.61°E	December 2024

Table 1: Deployment chronology and location of the stations from ICATMAR HFR network.

2.2 Technical characteristics

Catalonia's HFR network is based on CODAR's SeaSonde technology. This system was chosen because the Catalan coastline is highly rugged and the less rugged areas are subject to significant urban pressure. The system consists of a single antenna that functions both as a transmitter and receiver, along with a small-sized hut housing all the necessary electronics and software. The technology of this manufacturer has become the standard for measuring

surface ocean currents, thanks to its reliability and robustness.

Antenna's components:

- Compact antenna system of the Dome Style type with a monopole (the transmitter) and two orthogonal loops (together with the monopole, act as the receiver)
- Height: 6.4 m - Weight: 36 kg
- Data processing system: Apple Macmini computer and SeaSonde Radial Suite® software (release: R22 in CREU and BEGU, R23 in AREN, PBCN and GNST, and R24 in TOSS and SCAL)

Antenna's operating characteristics:

- Technology: backscatter with a direction-finding system to determine the signal direction of arrival.
- Operating frequency: 13.5 MHz in the band assigned by the *Secretaria d'Estat de Telecomunicacions i Infraestructures Digitals*.
- Range: measures are obtained in a radial distribution with respect the antenna's location over the bearing directions towards the sea, reaching more than 80 km offshore depending on environmental conditions.
- Resolution:
  - Spatial: 5° angular resolution and 1.5 km distance between range cells.
  - Temporal: measures are performed every 10 minutes and a datafile is generated hourly with the average estimation of measures taken from the past 75 min time interval.
- Communications: all HFR stations are equipped with a 4G industrial modem Sierra Wireless AirLink RV50X, except for the AREN station, which is connected through a fiber optic link.

2.3 APMs

Direction-finding radars consist of a compact design of one monopole and two orthogonal loops (Figure 3), whose phase path is common while the gains are different from each other in any direction. These characteristics allow to use the directional properties of the compact antenna to determine the direction of arrival of the sea echoes. The method used by CODAR antennas is the multiple signal classification (MUSIC) algorithm [Schmidt, 1986, Lipa et al., 2006].

Figure 3: Cross-loop antenna board from a CODAR 13.5 MHz station. Image provided by Qualitas Remos SL.

The directional properties of each SeaSonde HFR antenna have to be determined after their installation through a calibration method called antenna pattern measurement (APM), which allows the amplitude and phase determination of the antenna response as a function of the angle. Theoretically, the two crossed loops and the monopole have an ideal radiation pattern like the one in Figure 4 [Lai et al., 2017]. However, irregularities of the surrounding electromagnetic environment always modify the actual amplitude and phase patterns from that of the ideal reference. Therefore, the performance of the APM after the installation of the antennas in their final location and orientation allows to account for any factors such as ferromagnetic materials or other materials in the vicinity of the radar which may create interference with the antenna signal.

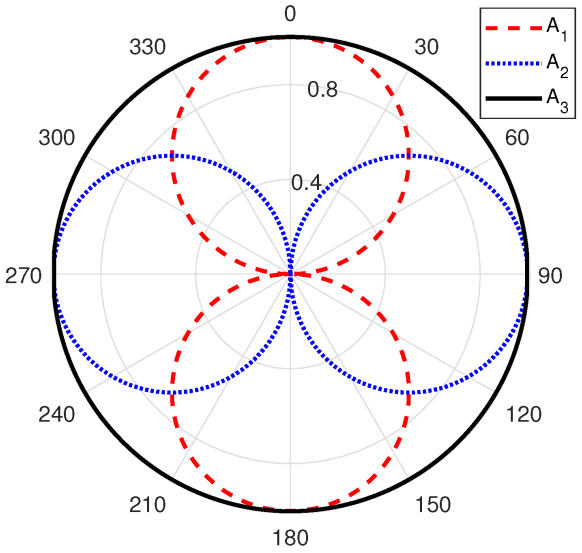

Figure 4: Representation of an ideal antenna pattern. The two orthogonal loops have cosine (A_1) and sine (A_2) radiation patterns relative to the monopole, and the monopole (A_3) gives an omnidirectional radiation pattern. Figure from Lai et al. [2017]

.

Calibration performance consist of collecting data emitted by a moving transponder in a boat with GPS tracker tracing an arc about 1 km offshore around the antenna. Derived APM data will determine the bearing of the calibrated antenna. Table 2 and Figure 5 gather the performing APM dates and their resulting geometries for the HFR ICATMAR network stations.

Station name	APM date	Inst. pattern date
CREU	07/03/2023 09:14	08/03/2023 11:20
BEGU	07/03/2023 12:49	08/03/2023 11:20
TOSS	03/06/2025 10:07	19/06/2025 09:00
AREN	29/02/2024 09:13	24/04/2024 09:20
PBCN	29/02/2024 14:37	14/06/2024 17:00
GNST	01/03/2024 09:11	25/04/2024 16:30
SCAL	-	-

Table 2: Chronology of the APM performance and implementation of the ICATMAR HFR stations (UTC time). At the publication of this report, the definitive APM for SCAL station is yet to be performed.

2.4 Available data

Datafiles and products supplied by the ICATMAR HFR network are differentiated between those generated by the *in situ* station software, SeaSonde Radial Suite® software from CODAR Ocean Sensors, and those generated by the ICATMAR own software. As a general practice, datafiles derived from an HFR network can be classified according to their processing levels (L), which are codified as: 0, 1A, 1B, 2A, 2B, 3A and 3B. This classification is based on the model proposed by JERICO-Next D5.14 and more information on that can be found in Quirós-Collazos et al. [2024b]. The particular characteristics of the ICATMAR HFRs processing chain and the data flow are described by Martínez [2023].

Files generated by the SeaSonde software correspond to processing levels from 0 to 2A. These are stored in duplicate (on the antenna's computer hard drive and on an external hard drive acting as a backup); the type of files generated by the antenna's internal software are listed below:

- CSQ and CSS spectra (`.cs` i `.css`), corresponding to L0 and L1 products
- Diagnoses (`.hdt, .rdt, .mdt i .xdt`)
- Ideal and measured radial velocities (`.ruv`), corresponding to L2A products
- Waves (`.wls`)

L2A radial velocity files are sent to two `sftp` server: the Geoblau server of the Generalitat de Catalunya and the ICATMAR server of the ICM-CSIC, through a `crontab` using `rsync` synchronization.

ICATMAR is the institution responsible of the management and generation of L2A, L2B, L3A and L3B data products from the ICATMAR HFR network. L2A and L2B products are `.ruv` format files which contain the radial velocity data measured by each antenna before and after data QC evaluation, respectively. L3A product is obtained after combination of

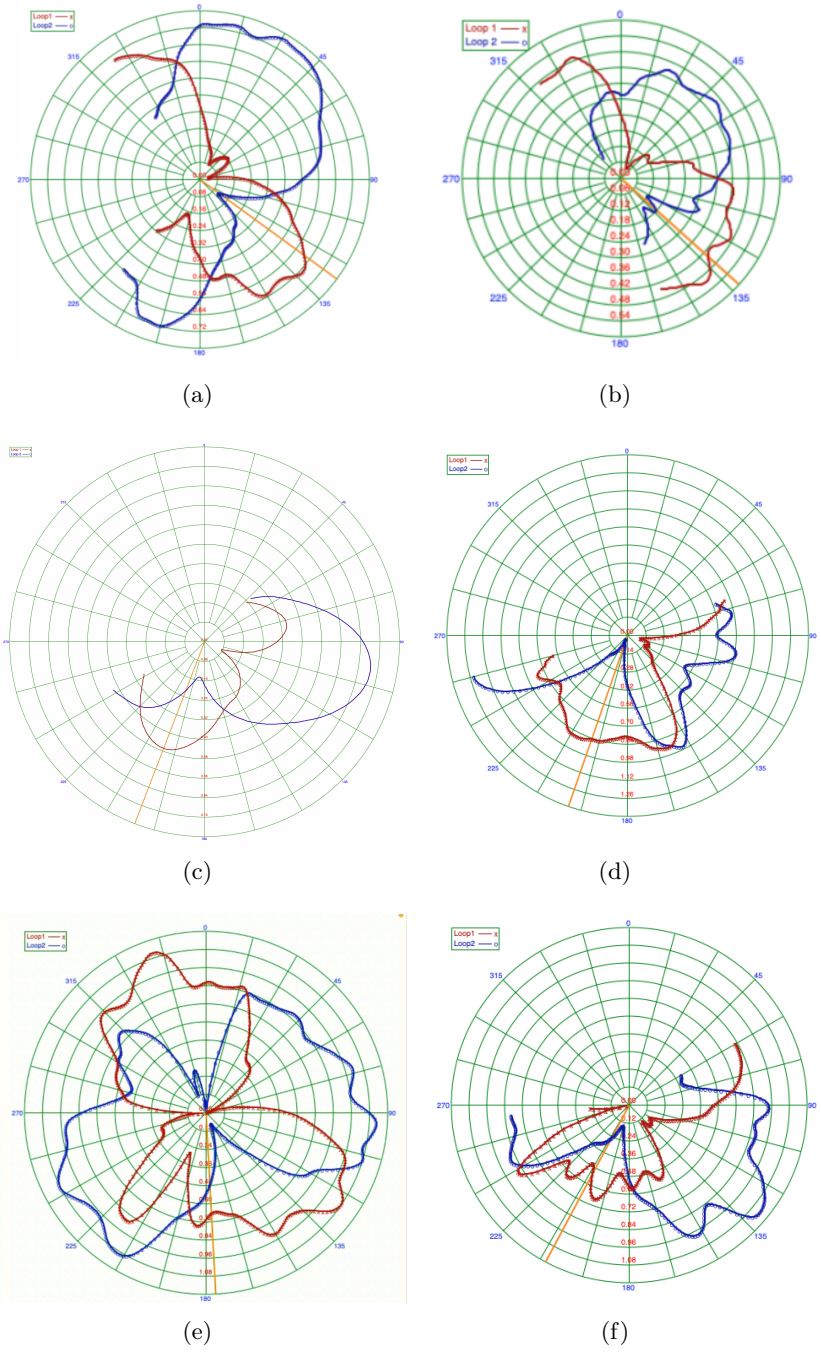

Figure 5: APMs of the ICATMAR HFR stations ordered from their north to south location along the Catalan coast: (a) CREU, (b) BEGU, (c) TOSS, (d) AREN, (e) PBCN and (f) GNST. At the publication of this report, the definitive APM for SCAL station is yet to be performed.

radial velocity data (L2B product) from different antennas to obtain 2D maps of total velocity data. Finally, L3B product correspond to the QC evaluation of L3A product. See examples of L2A, L2B, L3A products in the appendix A.

All these different level products were made available along the different phases of the ICATMAR HFR network deployment, thus increasing HFR coverage along the Catalan coast gradually. Table 3 sums up the chronology of data availability and the area of the Catalan coast that was covered at each stage.

Product	Station/Area	Data availability date
	CREU	17/02/2023 11:00
	BEGU	04/04/2023 08:00
	TOSS	06/06/2025 13:00
L2 (radials)	AREN	22/12/2023 11:00
	PBCN	22/12/2023 11:00
	GNST	22/12/2023 11:00
	SCAL	06/06/2025 13:00 (*)
	CATS (north)	04/04/2023 08:00
L3 (totals)	CATS (north + central)	22/12/2023 11:00
	CATS (all)	06/06/2025 13:00 (*)

Table 3: Chronology of the L2 and L3 data products availability derived from the ICATMAR HFR network (UTC time). Regarding CATS area, "*north*" refers to the northern sector of the Catalan coast where measures were taken by CREU and BEGU stations, "*central*" refers to the central sector where measures were taken by AREN, PBCN and GNST stations, and "*all*" refers to the whole Catalan coast covered by the complete array of antennas from the ICATMAR network (see Figure 1). Data availability date for SCAL is highlighted with the (*) symbol to indicate that data produced by that station is based on a provisional APM due to technical issues, currently under evaluation; for the same reason, the date from "CATS (all)", which is including data from SCAL, is also highlighted with the (*) symbol.

L2A and L3B data can be visualized on the ICATMAR website (`https://icatmar.cat/observacions/`) and, in particular, the latter are available for download. A detailed description of the different access modes to L3B data, as well as the content, structure and format of the datafiles is available in Quirós-Collazos et al. [2024b] technical report.

3 L2 products: radial velocity measures

The L2 products correspond to the HFR radial velocity data, this is, the radial current component towards an antenna georeferenced by the distance to the antenna and the clockwise angle from the North. In operational mode, the data processing chain produces, as mentioned, two products of radial data: L2A and L2B, where L2B contains the evaluation of a set of QC tests over the radial velocity data. Both types of data files are in ASCII format with the file extension `.ruv` (see examples in the appendix A).

L2A filenames follow the naming convention `RDLx_SSSS_YYYY_MM_DD_HH00.ruv`, where `RDL` identifies the type of file as a radial file and the `x` indicates the type of antenna pattern used (`m` for the measured antenna pattern and `i` for the ideal antenna pattern). `SSSS` is the four character identifying the station name. The date and time is indicated as `YYYY` (4 digits year), `MM` (2 digits month), `DD` (2 digits day), and `HH` (2 digits hour in a

24 hour format) using the Coordinated Universal Time (UTC). The file metadata and data content and structure is established at the configuration phase of the antennas and is broadly described in the CODAR's manufacturer LLUV file format specifications (available through their website `www.codar.com`) (see examples in appendix A).

L2B filenames keep the name of their corresponding L2A from which derive while adding `_l2b` at the end: `RDLm_SSSS_YYYY_MM_DD_HH00_l2b`.

3.1 Description of the Quality Control (QC) model

The QC model applied on the L2A data derived from the ICATMAR HFR network is based on the European common QC model for real-time HFR data [Corgnati et al., 2018] and the QC model developed by the US Integrated Ocean Observing System (US-IOOS) [US-IOOS, 2020].

The QC tests are manufacturer-independent and some of their associated threshold parameters have to be selected by each HFR operator depending on the antennas location and the historical knowledge or statistics derived from local sea characteristics.

The software developed by ICATMAR to execute the QC tests is described in the following section and is implemented in Python. This software uses methods from the public toolbox `HFRadarPy` [Smith et al., 2022] developed to read HFR files written in the CODAR Tabular Format (`CTF`).

QC flags criteria

Based on the flagging criteria used by the methods from the toolbox HFRadarPy [Smith et al., 2022], the flagging criteria applied for the L2A to L2B processing step is described in Table 4 and follows that described in US-IOOS [2020] which, in turn, is based on that adopted by UNESCO/IOC in 2013 [IOC-UNESCO, 2013].

Flag code	Meaning	Description
1	good data	The corresponding QC test has been passed
2	no QC performed	The corresponding QC test has not been evaluated
3	suspect data	These data should be used with caution
4	bad data	Data have failed one or more QC tests
9	missing value	-

Table 4: Quality control flag scheme applied for the quality assessment of radial velocity data, this is, L2B product.

QC tests

The applied QC tests are listed in Table 5 and they are the required ones for labelling the radial velocity data as L2B. Radial velocity measures are written as rows of a table where columns correspond to different variables containing information of the radial velocity measures. The result of the QC tests are added in consecutive columns to the main table, one column per test labelled accordingly, which means assigning a QC flag per test to each radial velocity measure (see examples in appendix A).

Two types of QC tests can be differentiated: those which evaluate the datafile and those which evaluate each single measure (see Table 5). Nonetheless, and despite the redundancy,

the results of QC tests evaluated over the datafile are informed in their corresponding table column with a flag for each measure (this is, the same flag value for each row).

QC test	Variable name (L2B files)	Scope of the test
Syntax	Q201	over file
Velocity threshold	Q202	over each velocity measure
Over-water	Q203	over each velocity measure
Radial count	Q204	over file
Median filter	Q205	over each velocity measure
Temporal derivative	Q206	over each velocity measure
Average radial bearing	Q207	over file
Overall flag	PRIM	over each velocity measure

Table 5: Set of quality control tests performed on radial velocity data (L2B files).

Syntax

This test evaluates the entire *.ruv* datafile and it assesses the proper formatting and the existence of all the necessary fields within the file. In particular:

- Check if timestamp is in the filename
- Table of radial measures must not be empty
- Metadata fields `FileType`, `Site`, `TimeStamp`, `Origin`, `PatternType` and `TimeZone` must be defined
- Filename timestamp must match the timestamp reported within the file
- Radial data table columns stated in the table description must match the actual number of columns reported for each row
- To ensure sure that site location makes sense: $-180 \leq lon \leq 180$ and $-90 \leq lat \leq 90$

Only if all these collection of tests are met correctly, the *Syntax* QC test is passed and, thus, value in Q202 variable is set to 1 in all velocity measures of that particular `.ruv` file. The method in the `HFRadarPy` toolbox is `qc_qartod_syntax` [Smith et al., 2022].

Velocity threshold

This test is performed over each measure evaluating if the module of radial velocity measures ($|u_r|$) are bigger than a maximum velocity threshold, which represents the maximum reasonable surface radial velocity for a given domain. The maximum velocity threshold for all the ICATMAR HFR network stations was set to 140 cm/s from a statistical analysis of the 2022 period of model-derived regional oceanographic data for the domain of the Catalan Sea (sourced from CMEMS [E.U. Copernicus Marine Service Information (CMEMS), 2019] and SOCIB [Juza et al., 2016]). This was a first approach due to the lack of HFR measurements for the region. We plan to review the threshold using the measured velocities.

The `HFRadarPy` toolbox has the method `qc_qartod_maximum_velocity` to handle it [Smith et al., 2022]. Internally, the algorithm takes into account two threshold levels, the "*high speed*" (u_{high}) and the "*maximum speed*" (u_{max}) with flags assigned as follows:

$$\begin{aligned} \text{If} \quad |u_r| < u_{high} &\Rightarrow Q202 \quad \text{flag} = 1 \text{ (good data)} \\ \text{If} \quad u_{high} < |u_r| < u_{max} &\Rightarrow Q202 \quad \text{flag} = 3 \text{ (suspect data)} \\ \text{If} \quad |u_r| > u_{max} &\Rightarrow Q202 \quad \text{flag} = 4 \text{ (bad data)} \end{aligned}$$

According with the criteria used by the final "*Overall flag*" test, velocity measures with flags 3 or 4 are not considered as "*good data*". In order to detect reasonable high velocities for the Catalan sea domain, we have set the following speeds thresholds:

$$u_{high} = 140 \text{ cm/s}, \; u_{max} = 170 \text{ cm/s}$$

However, only the first threshold u_{high} has a real effect on the performance of the *Velocity threshold* QC test.

Over-water

This test is performed over each measure evaluating if radial velocity measures are placed over land or in other unmeasurable areas (for example, behind an island or point of land). The method used, defined as `qc_qartod_valid_location_icatmar` is a modification of the original `qc_qartod_valid_location` from `HFRadarPy` toolbox. By default, the "*good data*" flag code 1 is assigned to Q203 variable for all velocity measures except for the following cases, where the "*bad data*" flag code 4 is assigned instead:

- Velocity measurements flagged value 128 in variable `VFLG`. This corresponds by default to the fifth column (denoted as `VectorFlag`) in the radial velocity table within all `.ruv` files. The value in this column is assigned by the CODAR Combine Grid software to indicate extra information about individual current vectors: particularly, value 128 indicates "*vector is out of bounds, for radial vectors this means that the vector was outside the Angular filter area*" (see CODAR LLUV file format specifications).
- Velocity measurements coordinates not located "on water" detected by the method `mask_over_land`.
- Particular bearings (θ, degrees clockwise from true North) and/or ranges (*rng*, distance from the antenna) from some stations that were not properly filtered by the two previous procedures:

– BEGU:

$$(\theta \leq 12° \vee \theta \geq 347°) \wedge rng > 40 \text{ km}$$

– CREU:

$$190° < \theta < 192° \wedge rng \geq 38.2776 \text{ km}$$
$$195° < \theta < 197° \wedge rng \geq 38.2776 \text{ km}$$

– AREN:

$$235° < \theta < 233° \wedge rng \geq 42 \text{ km}$$
$$238° < \theta \wedge rng \geq 13 \text{ km}$$

– PBCN:

$$41° < \theta < 43° \wedge rng \geq 19 \text{ km}$$
$$46° < \theta < 48° \wedge rng \geq 23 \text{ km}$$
$$51° < \theta < 53° \wedge rng \geq 48 \text{ km}$$

Radial count

This test evaluates the entire `.ruv` datafile assigning the "*bad data*" flag to all measures within the file if the total number of measures is lower than a threshold, since this scenario indicates a problem with data collection. If number of measures (N) is bigger than the threshold, all measures within the file are flagged as "*good data*".

The test is done by `qc_qartod_radial_count` method. Internally, the algorithm of this method takes into account two threshold levels, the "*low radial count*" ($N_{low} = 140$) and the "*minimum radial count*" ($N_{min} = 50$) with flags assigned as follows:

$$\begin{aligned} \text{If } N > N_{low} &\Rightarrow Q204 \quad \text{flag} = 1 \quad \text{(good data)} \\ \text{If } N_{min} < N < N_{low} &\Rightarrow Q204 \quad \text{flag} = 3 \quad \text{(suspect data)} \\ \text{If } N < N_{min} &\Rightarrow Q204 \quad \text{flag} = 4 \quad \text{(bad data)} \end{aligned}$$

According with the criteria used by the final "*Overall flag*" test, data flagged with 3 or 4 are not considered as "*good data*". Therefore, only the first threshold N_{low} has a real effect on the performance of the *Radial count* QC test. Based on that, the threshold criteria for N_{low} has been chosen following the default values set in `qc_qartod_radial_count` method for N_{min}, which is 150, but slightly looser.

Median filter

This test is performed over each measure ensuring that the measured radial velocity is not too different from nearby radial velocities. Method used is `qc_qartod_spatial_median` from `HFRadarPy` toolbox, which requires setting three threshold parameters:

- Range cell limit (RC_{lim}): which determines the size of the neighbourhood, in the range dimension, where to look for radial velocities, this is, over how many cells backward and forward look for neighbour radial velocities with respect to the cell being QC evaluated. Threshold value: $RC_{lim} = 2.1$, same as the default value used by the method.

- Angular limit ($\Delta\theta$): which determines the size of the neighbourhood, in the angular dimension, where to look for radial velocities, this is, over how many degrees around the evaluated cell look for neighbour radial velocities. Threshold value: $\Delta\theta = 10°$, same as the default value used by the method.
- Current difference (Δu_r, cm/s): which determines the acceptable level of discrepancy between the module of the evaluated radial velocity and the median value ($\mu_{1/2}$) obtained from the gathered velocities of the neighbourhood (the median include the point itself). Threshold value: $\Delta u_r = 30$ cm/s, same as the default value used by the method.

Accordingly, variable Q205 takes the following values:

$$\begin{aligned} &\text{If } \; ||u_r| - \mu_{1/2}| \leq \Delta u_r \;\Rightarrow\; Q205 \quad \text{flag} = 1 \quad \text{(good data)} \\ &\text{If } \; ||u_r| - \mu_{1/2}| > \Delta u_r \;\Rightarrow\; Q205 \quad \text{flag} = 4 \quad \text{(bad data)} \end{aligned}$$

Temporal derivative

This test is performed over each velocity measurement. It compares the values at a given time with those of the previous and next hours. Comparison is always performed between velocities measured at the same grid location. Since this method implies a one-hour delay in the data provision, the current hour file should have the related QC flag set to 2 (no QC performed) until it is updated to the proper values when the next hour file is generated.

The comparison is done computing the backward ($\partial_t^- u_r$) and forward differences ($\partial_t^+ u_r$) of speed values separated $\Delta t = 1h$:

$$\partial_t^- u_r = \left| \frac{u_r(t) - u_r(t - \Delta t)}{\Delta t} \right|, \qquad \partial_t^+ u_r = \left| \frac{u_r(t) - u_r(t + \Delta t)}{\Delta t} \right|, \quad \text{where} \quad \Delta t = 1h$$

In the `HFRadarPy` toolbox, such differences are checked against threshold values using the method `qc_qartod_temporal_gradient`. The algorithm takes into account two threshold levels: the "*temporal gradient warning*" (TG_{warn}) and the "*temporal gradient fail*" (TG_{fail}) with flags assigned as follows:

$$\begin{aligned} \text{If } \; (\partial_t^- u_r \wedge \partial_t^+ u_r) \leq TG_{warn} \;&\Rightarrow\; Q206 \text{ flag} = 1 \text{ (good data)} \\ \text{If } \; TG_{warn} < (\partial_t^- u_r \vee \partial_t^+ u_r) < TG_{fail} \;&\Rightarrow\; Q206 \text{ flag} = 3 \text{ (suspect data)} \\ \text{If } \; (\partial_t^- u_r \vee \partial_t^+ u_r) > TG_{fail} \;&\Rightarrow\; Q206 \text{ flag} = 4 \text{ (bad data)} \\ \text{If } \; \partial_t^- u_r \text{ or } \partial_t^+ u_r \text{ could not be estimated} \;&\Rightarrow\; Q206 \text{ flag} = 2 \text{ (no QC performed)} \end{aligned}$$

The last case usually happens either when anterior and posterior values are unavailable, or there are some missing data is present in a particular area or there are not good quality data, etc. Statistical analysis of model-derived regional oceanographic data of the 2022 period (sourced from CMEMS [E.U. Copernicus Marine Service Information (CMEMS), 2019] and SOCIB [Juza et al., 2016]) were used as a reference for the domain of the Catalan sea to determine the threshold values. This was a first approach due to the lack of HFR measurements for the region. As a result, temporal derivative thresholds were set to:

$$TG_{warn} = 30 \text{ cm/s/h}, \; TG_{fail} = 50 \text{ cm/s/h}$$

However, due to the criteria used by the final "*Overall flag*" test, velocity measures with flags 3 or 4 are not considered as "*good data*". As a result, only the first threshold TG_{warn} has a real effect on the performance of the *Temporal derivative* QC test.

Average radial bearing

This test evaluates the entire `.ruv` datafile. It checks that the average radial bearing ($\overline{\theta}$) calculated from all the measures contained in the datafile lies within a specified margin around the expected value of the antenna's normal operation. The margin has to be set according to site-specific properties. This test is applicable only to Direction Finding systems.

The method used is `qc_qartod_avg_radial_bearing` which takes into account the antenna's "*reference bearing*" (θ_{ref}) and two threshold levels, the "*warning threshold*" ($\Delta\theta_{warn}$) and the "*failure threshold*" ($\Delta\theta_{fail}$) with flags assigned as follows:

$$\begin{aligned} \text{If } |\overline{\theta} - \theta_{ref}| < \Delta\theta_{warn} &\Rightarrow Q207 \quad \text{flag} = 1 \text{ (good data)} \\ \text{If } \Delta\theta_{warn} \leq |\overline{\theta} - \theta_{ref}| < \Delta\theta_{fail} &\Rightarrow Q207 \quad \text{flag} = 3 \text{ (suspect data)} \\ \text{If } |\overline{\theta} - \theta_{ref}| \geq \Delta\theta_{fail} &\Rightarrow Q207 \quad \text{flag} = 4 \text{ (bad data)} \end{aligned}$$

Value assigned to both $\Delta\theta_{warn}$ and $\Delta\theta_{fail}$ thresholds is the same: 30°, which corresponds to the default $\Delta\theta_{fail}$ value used by the method. The "*reference bearing*", or value of normal operation, for each antenna is:

- CREU: $\theta_{ref} = 137°$
- BEGU: $\theta_{ref} = 74°$
- AREN: $\theta_{ref} = 156°$
- PBCN: $\theta_{ref} = 117°$ (except for files whose timestamp is previous to "2024-01-31_-2000", in which case $\theta_{ref} = 126°$)
- GNST: $\theta_{ref} = 161°$

Overall flag

For each radial velocity vector, this test evaluates the results of all the previous QC tests. It is defined as an overall QC variable, named `PRIM` in the L2B files, and the QC tests evaluation follows the next rule: it gets a "*good data*" flag if and only if all QC tests have been passed by that velocity measure, with the exception that QC test results with the "*no QC performed*" flag are ignored.

The test is performed using the method `qc_qartod_primary_flag` from `HFRadarPy` toolbox. Internally, the algorithm of this method assigns the flag code 1 to all measures, and then changes those whose any of the previous QC tests were labelled with 3 or 4 flag codes. Then, for each radial velocity measure the method works as follows:

- Step 1: by default ⇒ `PRIM` flag = 1 (good data)
- Step 2: if any Q201, Q202, Q203, Q204, Q205, Q206, Q207 = 3 ⇒ `PRIM` flag = 3 (suspect data)
- Step 3: if any Q201, Q202, Q203, Q204, Q205, Q206, Q207 = 4 ⇒ `PRIM` flag = 4 (bad data)

The flag results of this last QC test are important since only measurements that passed all the previous QC are flagged as "*good data*" (code 1) and taken into account for the total vector calculations.

3.2 QC statistics

The study period analysed in this report runs from 01/May/2023 00:00h to 30/April/2024 23:00h. During that time, CREU and BEGU stations were operating for a total of 8784 h, however, fewer L2A `.ruv` files were generated due to temporal antenna malfunctioning, station loss of GPS connection, etc.. Also, some of the L2A received files were corrupted, empty or did not have the proper formatting to be compiled to the next processing level, L2B (Table 6). For the analysis of the QC tests performance, L2B files not passing the Q201, Q204 or Q207 QCs tests (this is, those which evaluate the entire datafile, Table 5) have been discarded, as well as those not having the right dimensions to be concatenated with the rest of the L2B files (Table 6).

Station	Operating hours	L2A files	L2B files	L2B selected for QC analyses
CREU	8784	8129	8418	8001
BEGU	8784	8679	8283	8268

Table 6: Number of L2A `.ruv` files generated by CREU and BEGU stations and the resulting number of L2B files. Last column corresponds to the final number of L2B files that have been used for the analysis of the QC tests performance over 1 year data time-series. Percentages shown in Figures 6 and 7 are calculated over the number of L2B files indicated in the last column of this Table.

The results of the QC tests collection performance over the 1 year data time-series are presented in Figures 6 and 7, and are based on the analysis of datasets:

`RDLm_CREU_20230501_20240430_l2b.nc` and `RDLm_BEGU_20230501_20240430_l2b.nc`

which are a compilation of L2B files with dimensions being: time, range and bearing. Based on the file filtering process, 100% of the L2B files of the analysed datasets are flagged as "*good data*" (code 1) on the *Syntax* (Q201), *Radial count* (Q204) and *Average radial bearing* (Q207) QC tests, while percentages shown in Figures 6 and 7 of QC tests *Velocity threshold* (Q202), *Over-water* (Q203), *Median filter* (Q205) and *Temporal derivative* (Q206) are discussed in terms of that total number of L2B files passing the Q201, Q204 and Q207 QCs tests (Table 5).

The evaluation of *Velocity threshold* QC test shows that all radial velocities measured by both CREU and BEGU stations, over the study period, were below the threshold of 1.40 m/s (Figure 6a and 7a). That value was chosen based on the analysis of a 1 year time-series of sea surface velocity currents derived from SOCIB model [Juza et al., 2016]: particularly, the maximum velocity observed in 2022 dataset was taken as a reference, being well aware that it is a pretty high value. The aim was to be able to detect the complete variability of surface velocities across the HFR coverage areas, especially given the absence of prior HFR measurements in the studied region. Since currently more than 1 year time-series of HFR-derived sea surface currents is already available, future update to the QC model could adopt more region-specific velocity thresholds.

The evaluation of *Over-water* QC test shows that this tests is properly working by flagging as "*bad data*" those regions of the radial velocity grids that are in unmeasurable areas. For BEGU station, this is the case of measures located to the north of Cap de Creus. For CREU, this is the case of measures located to the south of Cap sa Sal and also measures placed in grid cells partially located on land along the coast of the Gulf of Lion. Figure 6b shows

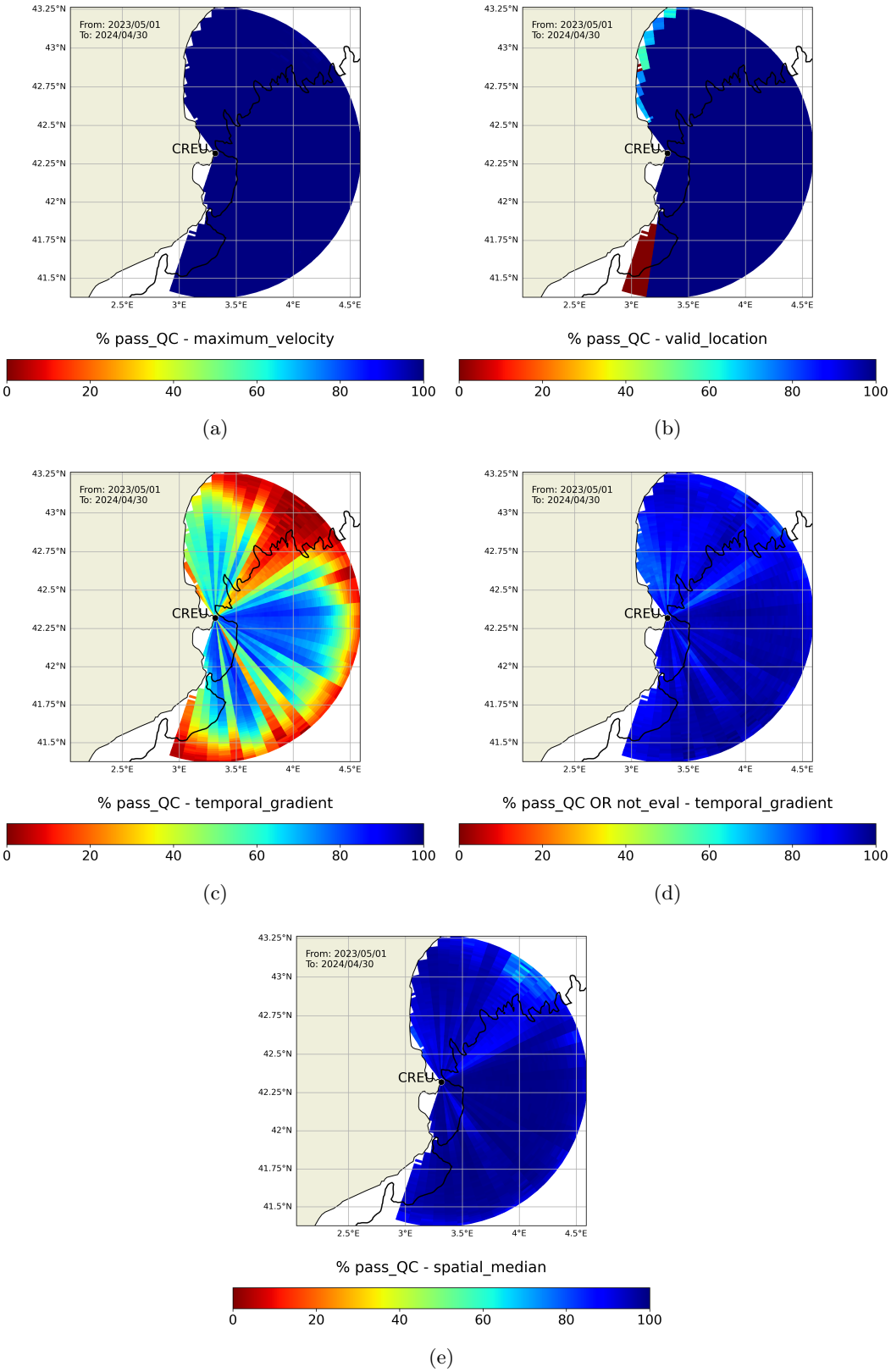

Figure 6: Percentage of radial velocity measures from CREU station that passed the (a) *Velocity threshold*, (b) *Over-water*, (c) *Temporal derivative* (d) *Temporal derivative* added to the number of cases when that particular QC test could not be evaluated, and (e) *Median filter* QC tests. Black contour line offshore indicates the location of the 200 m depth isobath.

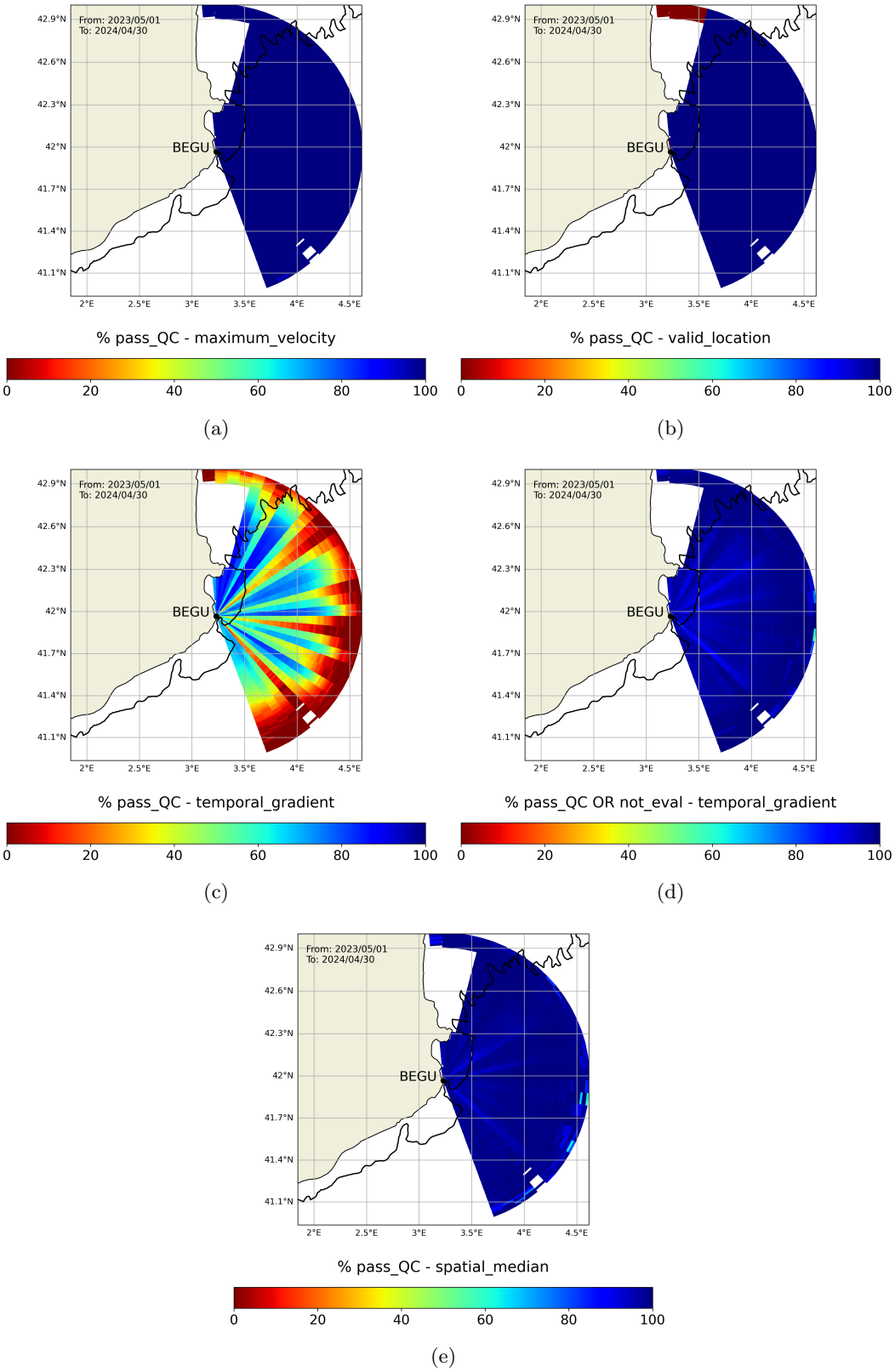

Figure 7: Percentage of radial velocity measures from BEGU station that passed the (a) *Velocity threshold*, (b) *Over-water*, (c) *Temporal derivative* (d) *Temporal derivative* added to the number of cases when that particular QC test could not be evaluated, and (e) *Median filter* QC tests. Black contour line offshore indicates the location of the 200 m depth isobath.

that around 70% of data from grid cells along the coast of the Gulf of Lion passed this QC test. This is because the algorithm was updated in March 2024 to achieve a more precise identification and discard of measures georeferenced on land grid cells.

Results on the *Temporal derivative* QC test evaluation are shown in Figures 6c-d (CREU) and 7c-d (BEGU). For both stations, panel (c) shows only the percentage of data where this test could be evaluated with a result of "*good data*" flag, while in panel (d) the percentage represents the proportion of data that either passed the *Temporal derivative* test or it could not be evaluated (basically due to the lack of previous, next or current hour measure at each location). Thus, we can conclude that the *Temporal derivative* test assessment is highly dependent on data availability, which is especially noticeable in the outer ranges of all directions and in some specific bearings (more notable in the north and north-east regions of the CREU station coverage area), which correspond to areas where data coverage is significantly lower.

Figures 6e and 7e show a good performance of the *Median filter* QC test with a rate of 80% or more of the data passing this test. The north and north-east regions of the CREU station coverage areas are the ones where data are less successful with this test (yet around the 80%), which are the same regions highlighted by the *Temporal derivative* QC test as regions with lower radial velocity measures. Nonetheless, the evaluation of this test performance indicates a good spatial coherence among the nearby radial velocity measures.

The performance of all QC tests are summarized by the *Overall flag* (PRIM) described in section 4.1. Plots in Figure 8 and 9 show the spatial distribution of data availability provided by each antenna's station (panel (a)), as well as the proportion of data passing the tests of the L2 QC model, based on the resulting *Overall flag* values (panel (b)). The actual percentage of good quality data measured by each station during the study period is shown in Figures 8c and 9c, for CREU and BEGU stations respectively, which ultimately will be the the radial velocity measures available for the total velocity current estimation. These results indicate that the QC assessment on radial velocity measures does not discard many data, which suggest that, when measures are produced they tend to be of good quality. However, the major limitation for total velocity estimation is the lack of measures, specially in the outer ranges of the antenna's coverage area, but also along all ranges of some specific bearings: 31°-51°, 151° in CREU and 47°-52°, 97°, 137° in BEGU stations. In this sense, Figure 10 shows that the effective measurement range in CREU and BEGU stations is 82.5 and 79.9 km, respectively, which is where the number of good quality observations falls below 50% of the total number of observations (this is, $N_{obs}/N_{max} \leq 0.5$).

3.3 General statistical assessment

Once radial velocity data (u_r) has been evaluated by the described QC model, those qualified as "*good data*" have been analysed to obtain general statistical properties by calculating the 1^{st} to the 4^{th} statistical moments and the PDF.

Moments and PDFs

Figures 11 and 12 show the spatial distribution of the 1^{st} to 4^{th} statistical moments, known as the *mean*, *standard deviation (std)*, *skewness* and *kurtosis*, respectively. They have been calculated for each cell of the radial grid over the time dimension for the aforementioned study period of 1 year. These results allow us detect general trends of radial velocity measures over the coverage area of stations CREU and BEGU.

According with map on the 1^{st} moment (Figures 11a and 12a), both stations detect a

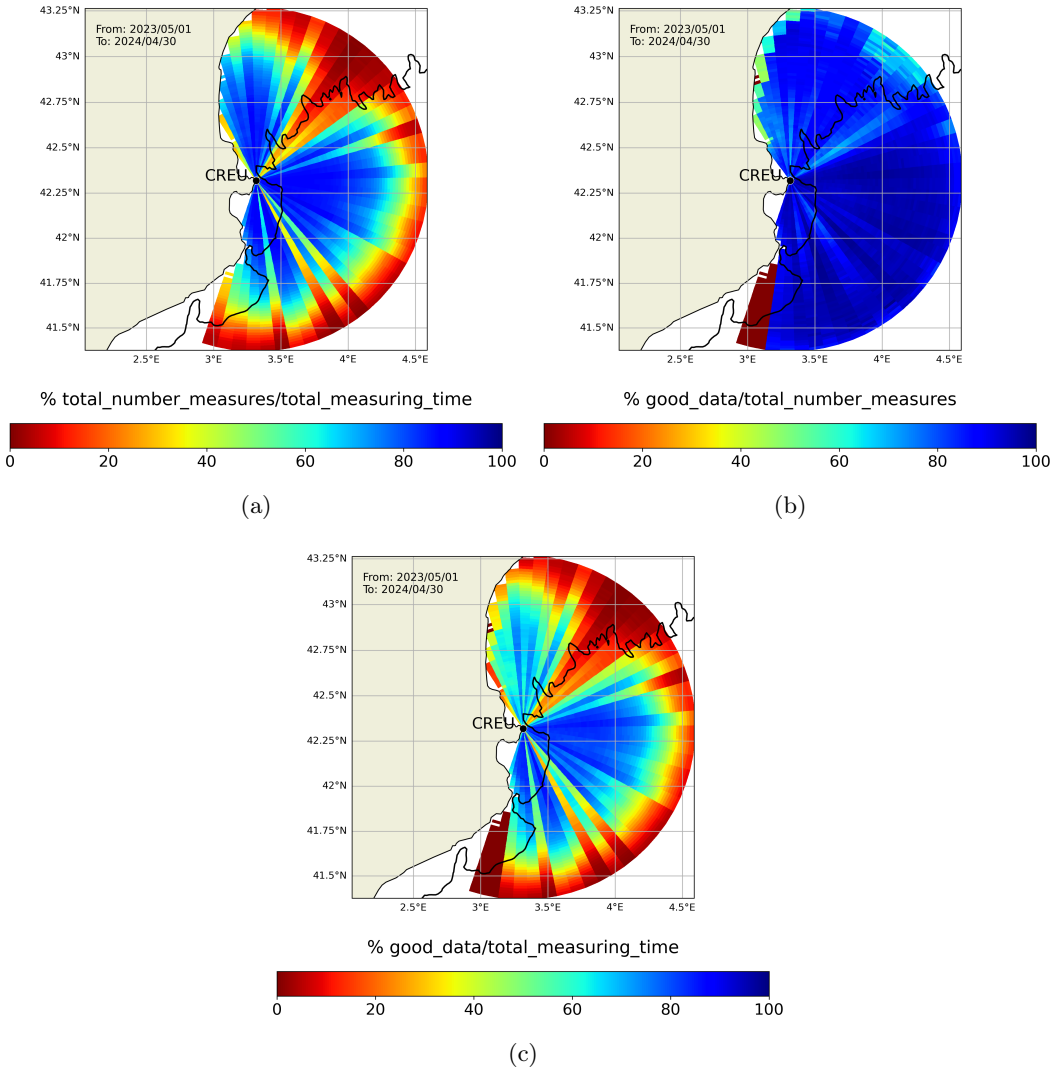

Figure 8: Assessment of radial velocity measures availability from CREU station before and after the QC performance: (a) *Total number of measures* (last column of Table 6) with respect the *Total measuring time* (second column of Table 6), (b) *Total number of measures flagged as "good data"* (which also includes those flagged as "*QC not evaluated*" by the *Temporal derivative* QC test) with respect the *Total number of measures* (last column of Table 6), (c) *Total number of measures flagged as "good data"* with respect the *Total measuring time* (second column of Table 6). Black contour line offshore indicates the location of the 200 m depth isobath.

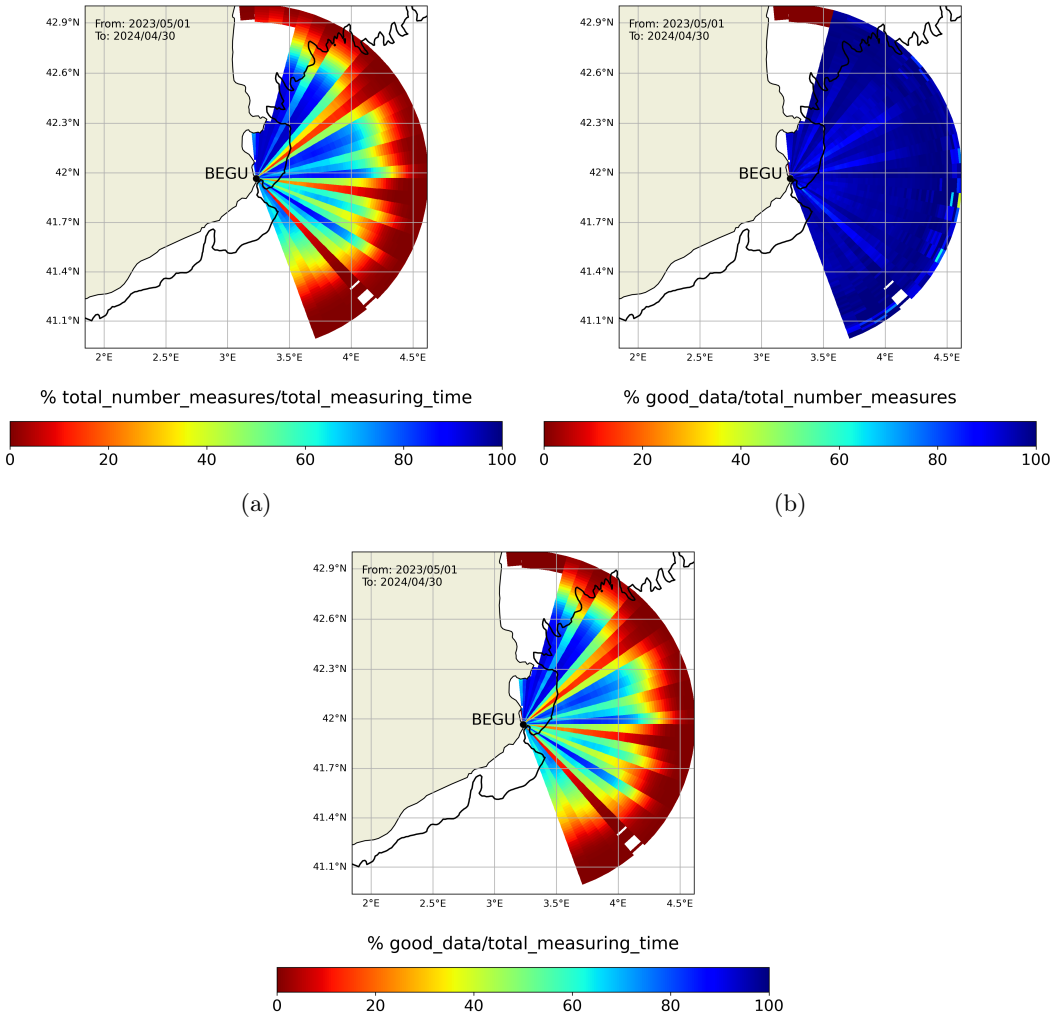

Figure 9: Assessment of radial velocity measures availability from BEGU station before and after the QC performance: (a) *Total number of measures* (last column of Table 6) with respect the *Total measuring time* (second column of Table 6), (b) *Total number of measures flagged as "good data"* (which also includes those flagged as "*QC not evaluated*" by the *Temporal derivative* QC test) with respect the *Total number of measures* (last column of Table 6), (c) *Total number of measures flagged as "good data"* with respect the *Total measuring time* (second column of Table 6). Black contour line offshore indicates the location of the 200 m depth isobath.

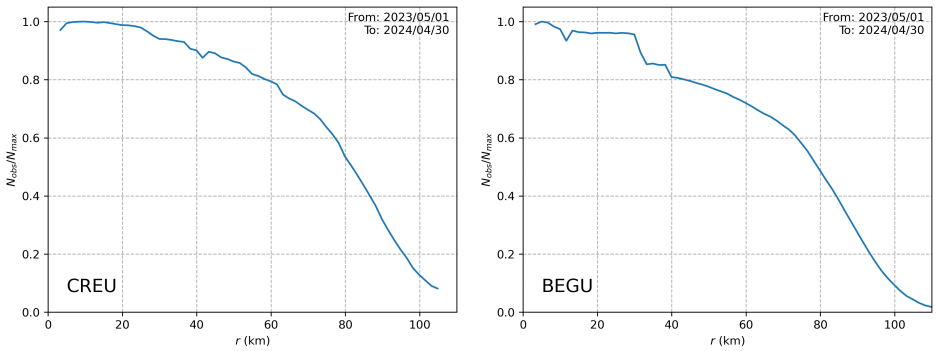

(a) (b)

Figure 10: Average variation of the number of "*good data*" measures (N_{obs}) with respect the distance (r) to (a) CREU and (b) BEGU stations, respectively. N_{obs} is normalized to the total number of "*good data*" measures for the study period (N_{max}). The average has been calculated along the time and bearing dimensions of the data distribution.

current flowing towards the antenna in the north-east area and a current flowing away the antenna in the south and south-east area of the coverage areas (corresponding to red and blue colours, for positive and negative mean u_r, respectively). This is in agreement with the known predominant current in this region, the Liguro-Provençal-Catalan current, which flows roughly from north-east to south-west along the continental shelf [Castellón et al., 1990].

2^{nd} to 4^{th} moments show roughly a radial pattern with some particularities. *std* maps show higher values at ranges closer to the antennas but also in the outer range crowns. CREU show also high values all along the northeastern bearings. Skewness and kurtosis also show higher positive values in the outer range crowns. Bearing in mind the data density plots in Figures 8 and 9, these trends might be caused by a lack of data in those areas, where stations could not measure more than 30% of "*good data*", likely resulting in more scattered and noisier data distributions there.

From mid to short range distances, on the other hand, *std*, *skewness* and *kurtosis* maps tell another story. *Skewness* values are around 0, while there is an excess *kurtosis* around the 0.5-1 interval. This is characteristic of turbulent flows, which show high variability with significant occurrence of extreme velocity values. PDFs from CREU and BEGU (Figure 13) are also in accordance with this interpretation, since PDFs are similar to the normal distribution in symmetry (as observed in the *skewness* maps) but with heavier tails, a characteristic feature of turbulent flows, and which denote a major occurrence of extreme u_r values.

PDFs also show that u_r values vary between -0.5 and 0.5 m/s most of the time in both CREU and BEGU stations. Moreover, CREU's PDF is slightly sharper and thinner than that from BEGU, thus indicating a slightly greater predominance of u_r values closer to 0, this is, less intense currents (Figure 13).

4 L3 products: total velocity measures

The L3 products correspond to the HFR total velocity data, this is, the total velocity component of the sea surface current. These are estimated by combining radial velocity measures from two or more antennas, measured over the same area and time. The method used for

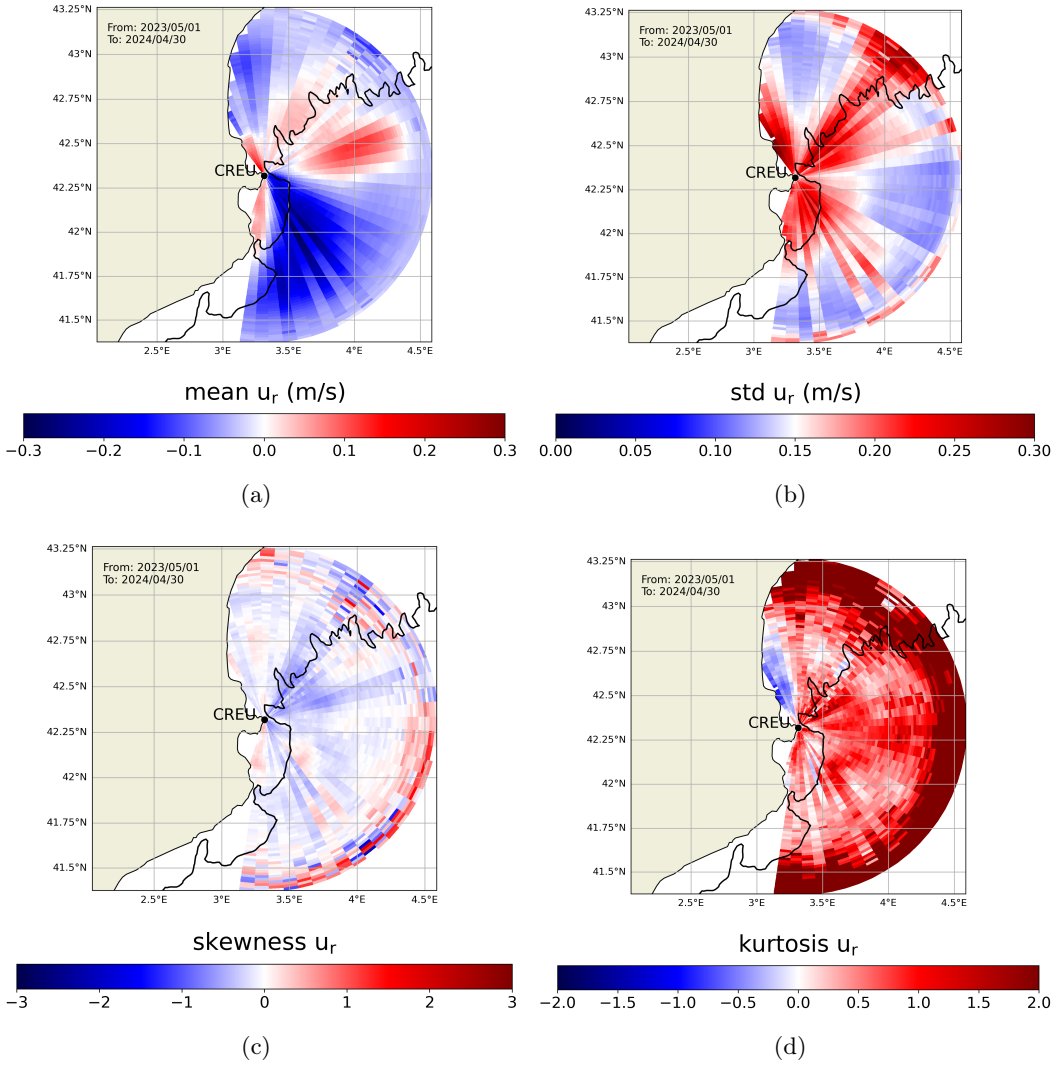

Figure 11: Spatial distribution of the 1^{st} to 4^{th} statistical moments estimated from radial velocities (u_r) measured by CREU station: (a) *mean*, (b) *standard deviation (std)*, (c) *skewness* and (d) Fisher *kurtosis* (where 0.0 is for a normal distribution). Calculation of moments have been done for each cell of the radial grid and over the time dimension for the 1-year period between the 01/May/2023 00:00h and the 30/April/2024 23:00h. Black contour line offshore indicates the location of the 200 m depth isobath.

4. L3 PRODUCTS: TOTAL VELOCITY MEASURES

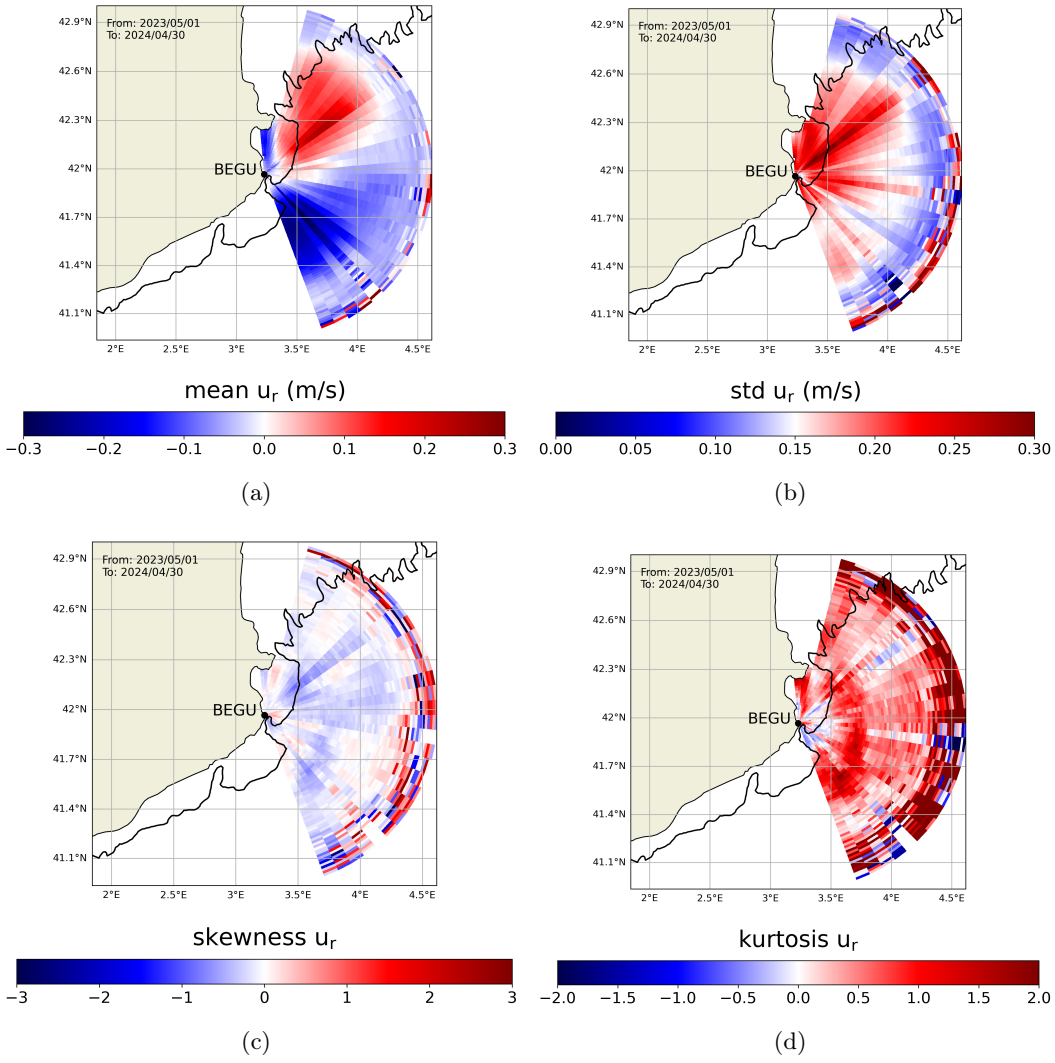

Figure 12: Spatial distribution of the 1^{st} to 4^{th} statistical moments estimated from radial velocities (u_r) measured by BEGU station: (a) *mean*, (b) *standard deviation (std)*, (c) *skewness* and (d) Fisher *kurtosis* (where 0.0 is for a normal distribution). Calculation of moments have been done for each cell of the radial grid and over the time dimension for the 1-year period between the 01/May/2023 00:00h and the 30/April/2024 23:00h. Black contour line offshore indicates the location of the 200 m depth isobath.

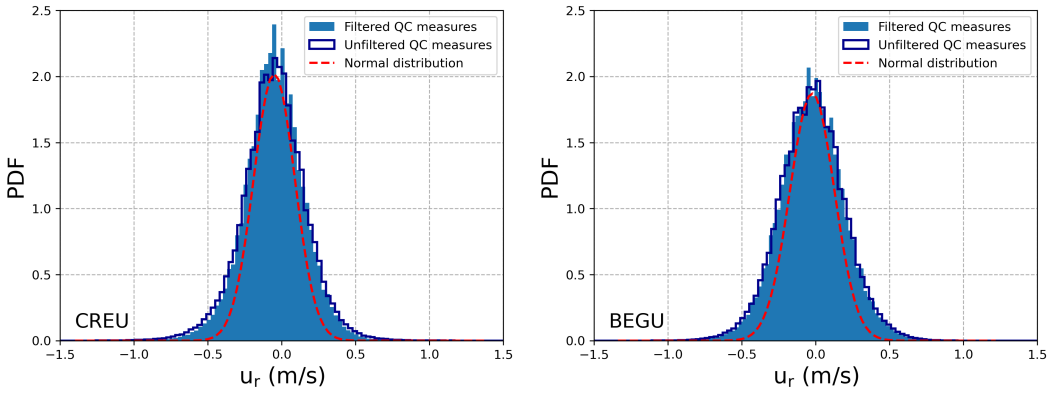

(a) (b)

Figure 13: Probability density functions (PDFs) of radial velocities (u_r) measured by (a) CREU and (b) BEGU stations. Blue filled bars and dark blue profiles correspond, respectively, to PDFs computed from measures passing the QC assessment (thus, from only "*good data*") and to PDFs computed from all measures before being evaluated by the complete QC assessment. Red dashed line depict the normal distribution associated to the "*good data*" dataset of each station.

the combination of radials is the unweighted least squares method (see Quirós-Collazos et al. [2024b] for a more detailed explanation). In operational mode, the data processing chain produces, as mentioned, two products of total velocity data: L3A and L3B, where L3B contains the evaluation of a set of QC tests over the total velocity data. L3A data files are in ASCII format with the file extension `.tuv` (see examples in appendix A), while L3B data files are in `netCDF` format with file extension `.nc`.

L3A and L3B filenames follow the naming convention `TOTL_SSSS_YYYY_MM_DD_HH00`. `TOTL` identifies the type of file as a file with total velocity data. `SSSS` is the four character identifying the area or region over which total velocity fields have been calculated, which in this case is CATS and refers to the Catalan sea region. The date and time is indicated as `YYYY` (4 digits year), `MM` (2 digits month), `DD` (2 digits day), and `HH` (2 digits hour in a 24 hour format) using the UTC time reference. L3A files metadata and data content and structure follow the CTF format described in the CODAR's manufacturer LLUV file format manual (see examples in appendix A). L3B files metadata and data content and structure is described in Quirós-Collazos et al. [2024b] manual. Unlike L2A and L2B files, L3A and L3B share the exact same filenames but with different file extension: `.tuv` and `.nc`, respectively.

4.1 Description of the QC model

The QC model applied on the L3A data derived from the ICATMAR HFR network is based on the European common QC model for real-time HFR data [Corgnati et al., 2018] and the QC model developed in US-IOOS [2020].

The QC tests are manufacturer-independent and some of their associated threshold parameters have to be selected by each HFR operator depending on the marine area being monitored, historical knowledge or statistics derived from local sea characteristics.

The software developed by ICATMAR to execute the QC tests described in the following section is implemented in Python.

QC flags criteria

The flagging criteria applied for the L3A to L3B processing step is described in Table 7 and follows that from the European common QC model described in Corgnati et al. [2018], which is based on the ARGO QC flag scale. This is different to the criteria used for the L2A to L2B processing step since there is no dependency on the toolbox `HFRadarPy` methods in the software developed by ICATMAR for the QC assessment on the L3A datafiles.

Flag code	Meaning	Description
0	no QC performed	The corresponding QC test has not been evaluated
1	good data	The corresponding QC test has been passed
2	probably good data	These data should be used with caution
3	potentially correctable bad data	These data are not to be used without scientific correction or re-calibration
4	bad data	Data have failed one or more QC tests
5	value changed	Data may be recovered after transmission error
6	value below detection	Data not used
7	nominal value	The provided value is not measured but comes from a priori knowledge (instrument design or deployment), e.g. instrument target depth
8	interpolated value	Missing data may be interpolated from neighbouring data in space or time
9	missing value	-

Table 7: Quality control flag scheme applied for the quality assessment of total velocity data, this is, L3B product.

QC tests

The applied QC tests are listed in Table 8 and they are the required ones for labelling the total velocity data as L3B. The result of each QC test is represented as an additional variable in the L3B `.nc` files, which contain a flag related to each data vector of the total velocity field on that datafile. These variables are 3D matrices with the same dimensions as those of the velocity data variables, which are *time*, *depth*, *latitude* and *longitude* (*time* and *depth* dimensions are both of size 1, since total velocity fields in each datafile correspond to a certain time instant and a single surface data layer of 1 m depth). See section 6.2 in Quirós-Collazos et al. [2024b] for a detailed description on the `netCDF` file structure and data variables.

An overall QC variable, named *qcflag* in the L3B files, sums up the results of all the QC tests evaluated over a a total velocity vector based on the next rule: it gets a "*good data*" flag (this is, flag code 1) if and only if all QC tests have been passed by that velocity measure, with the exception that QC test results with the "*no QC performed*" flag (this is, flag code 0) are ignored.

QC test	Variable name in L3B files	Type of test evaluation
Data density threshold	ddns_qc	over each velocity measure
Velocity threshold	cspd_qc	over each velocity measure
Temporal derivative	vart_qc	over each velocity measure
GDOP threshold	gdop_qc	over each velocity measure
Overall flag	qcflag	over each velocity measure

Table 8: Set of quality control tests performed on total velocity data.

Data density threshold

This test is performed over each measure to ensure that a minimum number of radial vectors ($N_{radials}$) have been used to compute each total velocity vector. $N_{radials}$ is calculated by adding the number of radials from each antenna that have been involved in the estimation of a total velocity vector. A parameter is defined in the algorithm to set the threshold value as:

$$\texttt{min\_nrad\_contr} = 3$$

This value is set to follow the criteria used by the the European common QC model for real-time HFR data [Corgnati et al., 2018].

Accordingly, flags are assigned as follows:

$$\begin{aligned} \text{If } N_{radials} > \texttt{min\_nrad\_contr} &\Rightarrow \texttt{ddns\_qc} \text{ flag} = 1 \text{ (good data)} \\ \text{If } N_{radials} \leq \texttt{min\_nrad\_contr} &\Rightarrow \texttt{ddns\_qc} \text{ flag} = 4 \text{ (bad data)} \end{aligned}$$

Velocity threshold

This test is performed over each measure evaluating if the module of total velocity vectors ($|U|$) are bigger than a maximum velocity threshold, which represents the maximum reasonable surface total velocity for a given domain. The threshold value was set following the same criteria used for the radials *Velocity threshold* QC test, this is, based on the statistical analysis of the 2022 period of model-derived regional oceanographic data (sourced from CMEMS [E.U. Copernicus Marine Service Information (CMEMS), 2019] and SOCIB [Juza et al., 2016]) performed for the domain of the Catalan sea.

A parameter is defined in the algorithm to set the threshold value as:

$$\texttt{max\_speed} = 1.7\ m/s$$

Accordingly, flags are assigned as follows:

$$\begin{aligned} \text{If } |U| < \texttt{max\_speed} &\Rightarrow \texttt{cspd\_qc} \text{ flag} = 1 \text{ (good data)} \\ \text{If } |U| \geq \texttt{max\_speed} &\Rightarrow \texttt{cspd\_qc} \text{ flag} = 4 \text{ (bad data)} \end{aligned}$$

Temporal derivative

This test is performed over each velocity measure. It compares the module of the total velocity vector ($|U|$) of the current hour with that of the previous hour. Comparison is

always performed between total velocities at the same latitude and longitude coordinates of the grid. Different from the radials *Temporal derivative* QC test, this implementation allows to evaluate this QC test in operational mode, since it not requires to wait for the next hour file for it to be evaluated.

The test is assessed by calculating the difference between current and previous hour velocity measures ($\partial_t^- |U|$) as follows:

$$\partial_t^- |U| = \left| \frac{|U(t)| - |U(t-\Delta t)|}{\Delta t} \right|, \text{ where } \Delta t = 1\text{h}$$

Then, the difference is compared with a threshold value, which is defined in the algorithm as: `grdtfl` from "*gradient temporal fail*". The algorithm assigns flags as follows:

$$\begin{aligned} \text{If } \partial_t^- |U| < \texttt{grdtfl} &\Rightarrow \texttt{vart\_qc} \text{ flag} = 1 \text{ (good data)} \\ \text{If } \partial_t^- |U| \geq \texttt{grdtfl} &\Rightarrow \texttt{vart\_qc} \text{ flag} = 4 \text{ (bad data)} \\ \text{If } \partial_t^- |U| \text{ could not be estimated} &\Rightarrow \texttt{vart\_qc} \text{ flag} = 0 \text{ (no QC performed)} \end{aligned}$$

The latest case occurs when the file of previous hour is not available, or there are some missing data or not good quality data in a particular area, etc. As for radials, statistical analysis of the 2022 period of model-derived regional oceanographic data (sourced from CMEMS [E.U. Copernicus Marine Service Information (CMEMS), 2019] and SOCIB [Juza et al., 2016]) were performed for the domain of the Catalan sea to determine this threshold. This was a first approach due to the lack of HFR measurements for the region. As a result, the temporal derivative threshold was set to:

$$\texttt{grdtfl} = 0.5\ m/s/h$$

GDOP threshold

This test is performed over a variable called `gdop` (Geometrical Dilution Of Precision, GDOP), which is a coefficient of uncertainty that characterizes the effect of the geometry of the combined radar sites on the measurements accuracy and position determination errors [Trujillo et al., 2004]. Particularly, as the combining radial vectors deviate from orthogonality GDOP values increase.

Since a GDOP value is estimated for each total velocity vector, this QC test assesses whether estimated GDOP values are not bigger than a maximum threshold. A parameter is defined in the algorithm to set the threshold value as:

$$\texttt{max\_gdop} = 2$$

This value is set to follow the criteria used by the the European common QC model for real-time HFR data [Corgnati et al., 2018].

Accordingly, flags are assigned as follows:

$$\begin{aligned} \text{If } \texttt{gdop} < \texttt{max\_gdop} &\Rightarrow \texttt{gdop\_qc} \text{ flag} = 1 \text{ (good data)} \\ \text{If } \texttt{gdop} \geq \texttt{max\_gdop} &\Rightarrow \texttt{gdop\_qc} \text{ flag} = 4 \text{ (bad data)} \end{aligned}$$

Overall flag

For each total velocity vector, this test evaluates the results of all the previous QC tests. It is defined as an overall QC variable, named `qcflag` in the L3B files, and the QC test evaluation follows the next rule: it gets a "*good data*" flag if and only if all QC tests have been passed by that velocity measure, with the exception that QC test results with the "*no QC performed*" flag are ignored. The algorithm assigns flags as follows:

If $[\texttt{ddns\_qc} + \texttt{cspd\_qc} + \texttt{vart\_qc} + \texttt{gdop\_qc}] \leq 4 \Rightarrow$ `PRIM` flag = 1 (good data)

If $[\texttt{ddns\_qc} + \texttt{cspd\_qc} + \texttt{vart\_qc} + \texttt{gdop\_qc}] > 4 \Rightarrow$ `PRIM` flag = 4 (bad data)

4.2 QC statistics

The study period analysed in this report runs from 01/May/2023 00:00h to 30/April/2024 23:00h, meaning that the ICATMAR HFR network was operating for a total of 8784 h. However, as mentioned in section 3.2, different issues caused that not all HFR antennas were operating or producing good radial velocity data simultaneously to allow the calculation of total velocity fields for that whole period. Table 9 summarizes the number of L3A (`.tuv`) and L3B (`.nc`) files generated by the ICATMAR HFR network during the period analysed for this report.

HFR network	Operating hours	L3A generated files	L3B generated files	L3B files used for the QC analyses
ICATMAR	8784	7975	7956	7956

Table 9: Number of L3A `.tuv` and L3B `.nc` files generated by the ICATMAR HFR network for the period analysed in this report. Last column corresponds to the final number of L3B files that have been used for the analysis of the QC tests performance over 1 year data time-series. Percentages shown in Figure 14 are calculated over the number of L3B files indicated in the last column of this Table.

In Figure 14 we show the results of the performance of the QC tests collection over the data time-series compiled in the `TOTL_CATS_20230501_20240430_l3b.nc` file. Percentages shown in the figure are discussed in terms of the total number of L3B files indicated in last column of Table 9, which represent the 100%. Note that only total velocity fields derived from CREU and BEGU stations have been taken into account for the analysed period.

Figure 14a shows the result of evaluating the *Data density threshold* QC test, which indicates that at least 3 radial velocity measures were available for total velocity estimations most of the time. Slightly less occurrence of this condition is observed in the northern and southernmost regions of the coverage area, with a rate of <80-90% of total velocities passing this QC test.

Regarding the *Velocity threshold* QC test, Figure 14b shows that, for the analysed period, absolute values of almost 100% of total velocities were below the 1.7 m/s threshold, with only very few velocity vectors being discarded by this QC test from the northern and southernmost regions of the coverage area. This is an expected result since the chosen threshold value was high in order to detect the whole range of total velocity variability of the region. As for the *Velocity threshold* QC test set for radials, the current 1 year time-series analyse will allow to adjust the velocity threshold more in accordance with the oceanographic characteristics of this region.

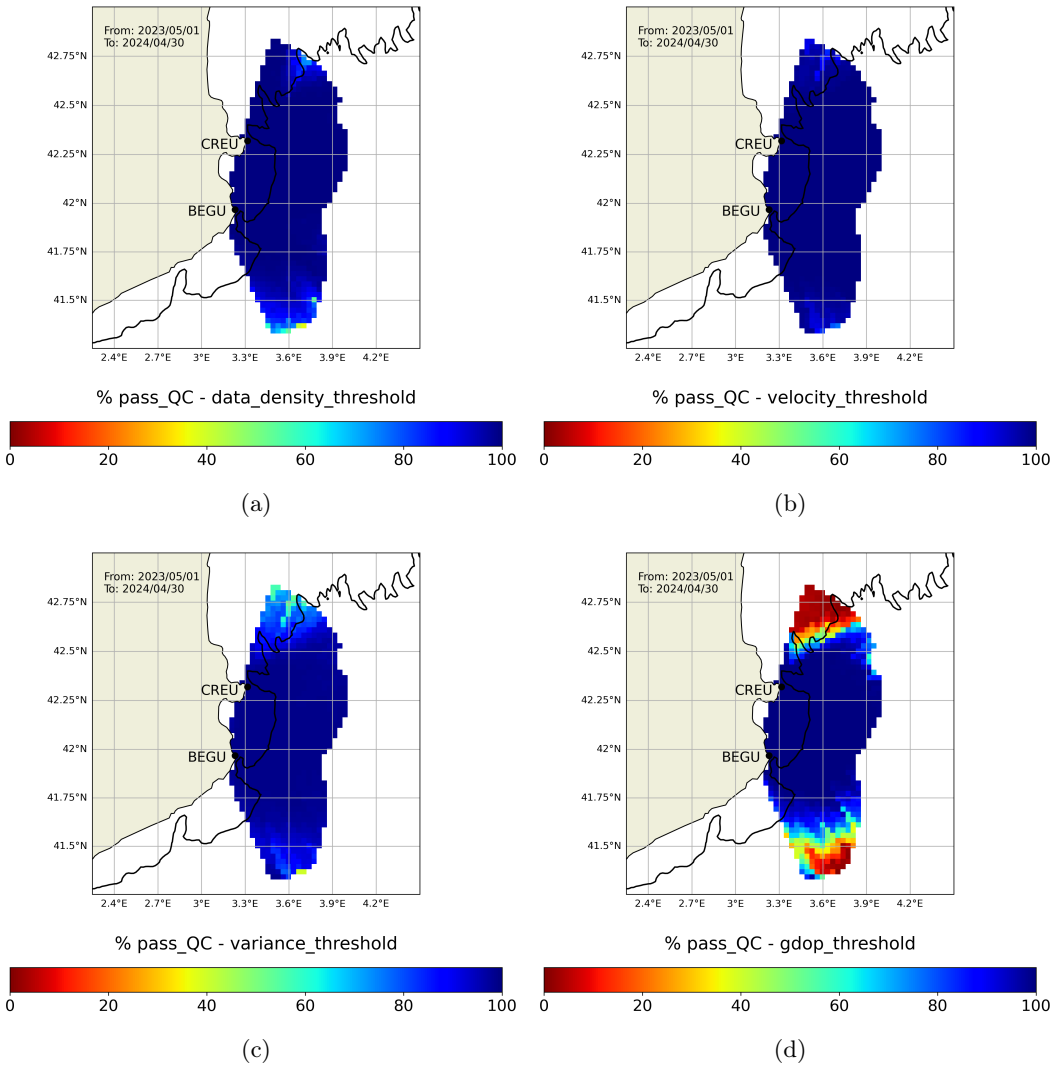

Figure 14: Percentage of total velocity vectors that passed the (a) *Data density threshold*, (b) *Velocity threshold*, (c) *Temporal derivative* and (d) *GDOP threshold* QC tests. Black contour line offshore indicates the location of the 200 m depth isobath and black dots indicate the location of CREU and BEGU stations.

Similar to the previous two QC tests, velocity vectors from northern and southernmost regions of the coverage area were the less successful in passing the *Temporal derivative* QC, with a pass rate of <70% in the far north of the coverage area (Figure 14c).

Lastly, the *GDOP threshold* QC test seems to be the more restrictive of the L3 QC collection. North of the 42.5°N and south of the 41.6°N latitudes, roughly less than 50% of velocity vectors pass the *GDOP threshold* test, with a rate below 10% in the far north and south of the coverage area (Figure 14d).

The result of all QC tests is summarized by the *Overall flag* (`qcflag` variable), which discriminates total velocity vectors as "*good data*" or "*bad data*". The percentage of good quality data is shown in Figure 15b, which indicates that, for the analysed period, the best HFR-derived total velocity data were obtained between the 41.6°N and 42.5°N latitudes of the monitored marine area. Additionally, Figure 15a presents the data density distribution produced by the ICATMAR HFR network over the study period. This shows a major lack of data in the northern and, more significantly, southernmost regions of the coverage area, and also in some particular directions which likely correspond to bearings from CREU and BEGU station with a systematic loss of radial measurements (see Figures 8a and 9a).

Figure 15c is the combination of results from Figures 15a and 15b, which is the "*good data*" density distribution produced by the ICATMAR HFR network over the study period. It shows that good quality total velocities are mainly obtained between the 41.6°N and 42.5°N latitudes of the coverage area. North of 42.5°N, the lack of good data is largely caused by data discarding due to the QC assessment (specially by the *GDOP threshold* test), while south of 41.6°N the lack of good data results from the combination of data discarding by the QC assessment and low number of velocity vectors obtained in that region. East of about 3.7-3.8°E and offshore CREU station, the lack of good data is mainly caused by systematic loss of radial measurements from BEGU station around the 47-52° bearings (see Figure 9a).

4.3 General statistical assessment

After the evaluation of total velocity data (U) by the described QC model, those qualified as "*good data*" have been analysed to obtain general statistical properties, such as the 1^{st} to the 4^{th} statistical moments, the eddy kinetic energy (EKE) and the PDF.

Moments, EKE and PDFs

Figures 16 and 15 show the spatial distribution of the 1^{st} to 4^{th} statistical moments, known as the *mean*, *standard deviation (std)*, *skewness* and *kurtosis*, respectively, as well as the *EKE*. They have been calculated for each cell of the grid from total velocity estimations, over the time dimension, this is, for the aforementioned study period of 1 year. These results allow to detect general trends of total velocity measures over the coverage area.

The maps on the 1^{st} moment have been calculated for the u and v components of the total velocity U, and for its module $|U|$ (Figure 16). The results show that zonal and meridional components of the monitored surface currents were predominantly positive (this is, eastward) and negative (this is, southward), respectively, thus resulting in an average surface current which flows to the south and slightly advects to the south-east and east in the coverage area, south of the 41.75°N latitude. While the general tendency is in agreement with the known predominant current in this region (the Liguro-Provençal-Catalan current, which flows roughly from north-east to south-west along the continental shelf [Castellón et al., 1990]), the flow advection to the south-east detected south of the 41.75°N latitude and the apparently 0

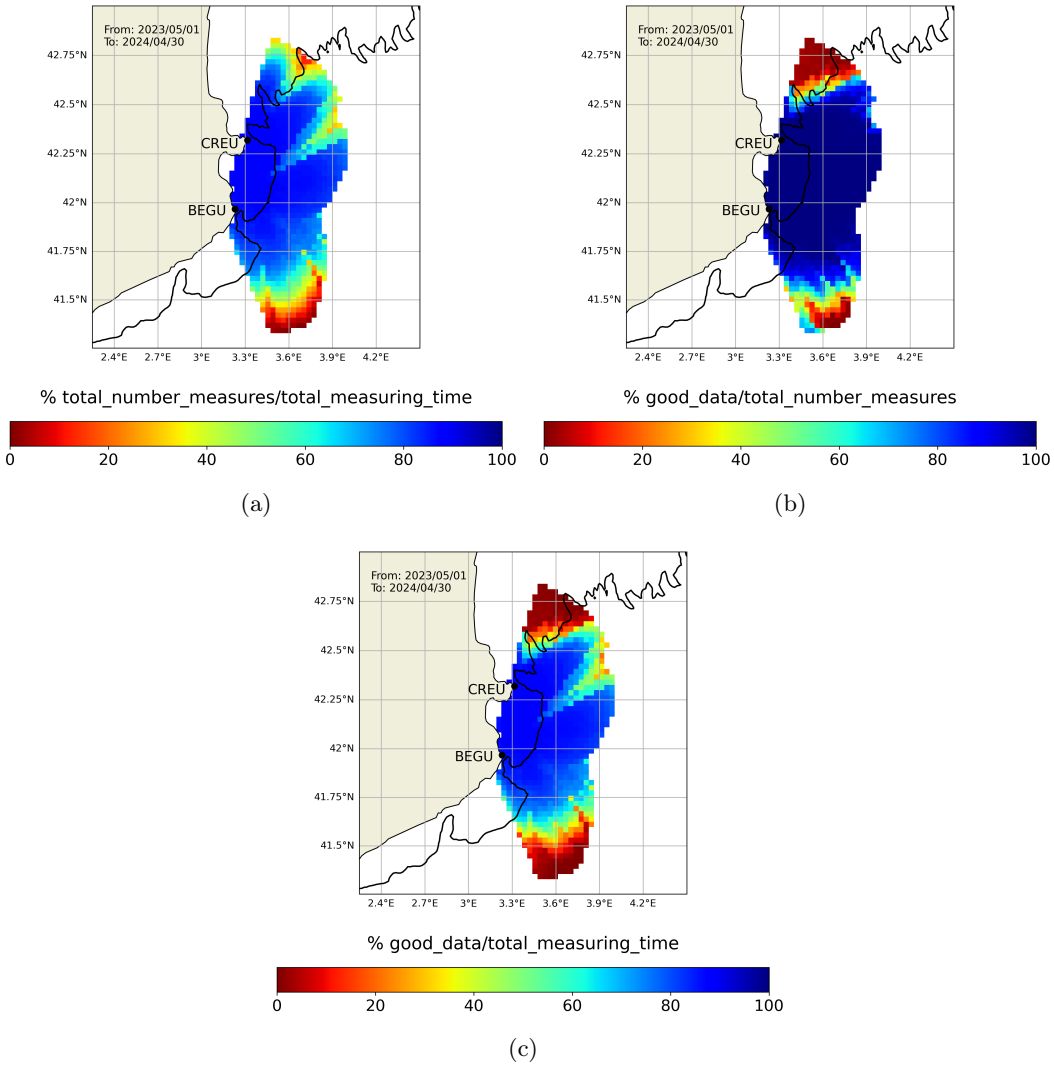

Figure 15: Assessment of estimated total velocity vectors (referred in this figures as "*measures*") derived from the ICATMAR HFR network before and after the QC performance: (a) *Total number of measures* (last column of Table 9) with respect to *Total measuring time* (second column of Table 9), (b) *Total number of measures flagged as "good data"* with respect the *Total number of measures* (last column of Table 9), (c) *Total number of measures flagged as "good data"* with respect to the *Total measuring time* (second column of Table 9). Black contour line offshore indicates the location of the 200 m depth isobath and black dots indicate the location of CREU and BEGU stations.

m/s flow over the continental shelf north of Cap de Creus, are both unexpected results. They coincide in location with areas with the lowest density of good quality data (Figure 15c), thus, the addition of more data to the time series, and complementing it with measurements from later-installed antennas (see sections 2.1 and 2.4), will help elucidate the interpretation of these preliminary results.

Regarding the map on the 2^{nd} moment (Figure 17a), it shows that *std* values are quite homogenous around 0.15 m/s within the area of higher density of good quality data, while they increase towards the north and south of the coverage area, which coincide with areas where the number of good data starts to decrease (see Figure 15b). However, the highest variability values in the north also coincides with the continental slope location, where gravity-driven deep-water processes are more likely to occur. Extending the time series and data coverage area will help distinguish the causes behind these detected high variability regions. The *std* values close to 0 m/s in the far north and south are likely the result of very few data density with very small total velocity modules (almost 0 m/s, see Figures 15 and 16).

The maps on the 3^{rd} and 4^{th} moments (Figure 17b-c) show and excess *skewness* and *kurtosis*. It should be taken into account they are derived from the total velocity module $|U|$, this is, all positive values which do not follow a gaussian distribution. The *skewness* map is pretty homogenous with values around 1-1.5, thus suggesting that the majority of data points are concentrated on the left side of the distribution, where total velocity values are smaller (this is, closer to 0 m/s). The *kurtosis* map shows the predominance of excess kurtosis, which could be related to a higher probability of occurrence of extreme values in this region.

Lastly, the *EKE* map (Figure 17d) shows a profile of low energy (<0.04 m^2/s^2) in the area of higher good data density (see Figure 15b), while the highest energy coincides with regions of high variability (*std*, Figure 17a) and highest $|U|$ (Figure 16c); however *EKE* plummets in the far north and south regions of the coverage area were *std*, mean $|U|$ and good data density are the lowest. As mentioned for the *std* map, more data will be needed to confirm or discard whether the apparently more dynamic marine areas are so or they are spurious results caused by a lower data density.

PDFs have been calculated for the u and v components of total velocity (Figure 18). In both cases, PDF shape is similar to the normal distribution in symmetry but with heavier tails, a characteristic feature of turbulent flows, which are associated with major occurrence of extreme values. Also, as observed for radials in Figure 13, PDFs of total velocity components, u and v, show that values vary between -0.5 and 0.5 m/s most of the time. They are also in accordance with *mean* u and v maps (Figure 16a-b), since PDF and associated normal distribution peaks fall within small positive values, in the case of the u component, and slightly more offset from 0 and towards negative value, in the case of the v component.

4.4 Data validation

For data validation, the 1-year long time series of sea surface velocities measured by the ICATMAR HFR has been compared with Eulerian velocity measurements from a mete-ocean buoy moored in the marine region off Begur (hereafter, Begur buoy) belonging to Puertos del Estado. Secondly, data derived from a search and rescue (SAR) testing exercise, which was also performed within the area covered by the HFR network, was analysed in order to assess the ability to reproduce Largrangian trajectories of drifting objects using current data derived from the ICATMAR HFR network.

Begur buoy (41.92°N, 3.67°E, mooring depth 1200 m) is located within the coverage area monitored by the ICATMAR HFR network and where optimal data density of good

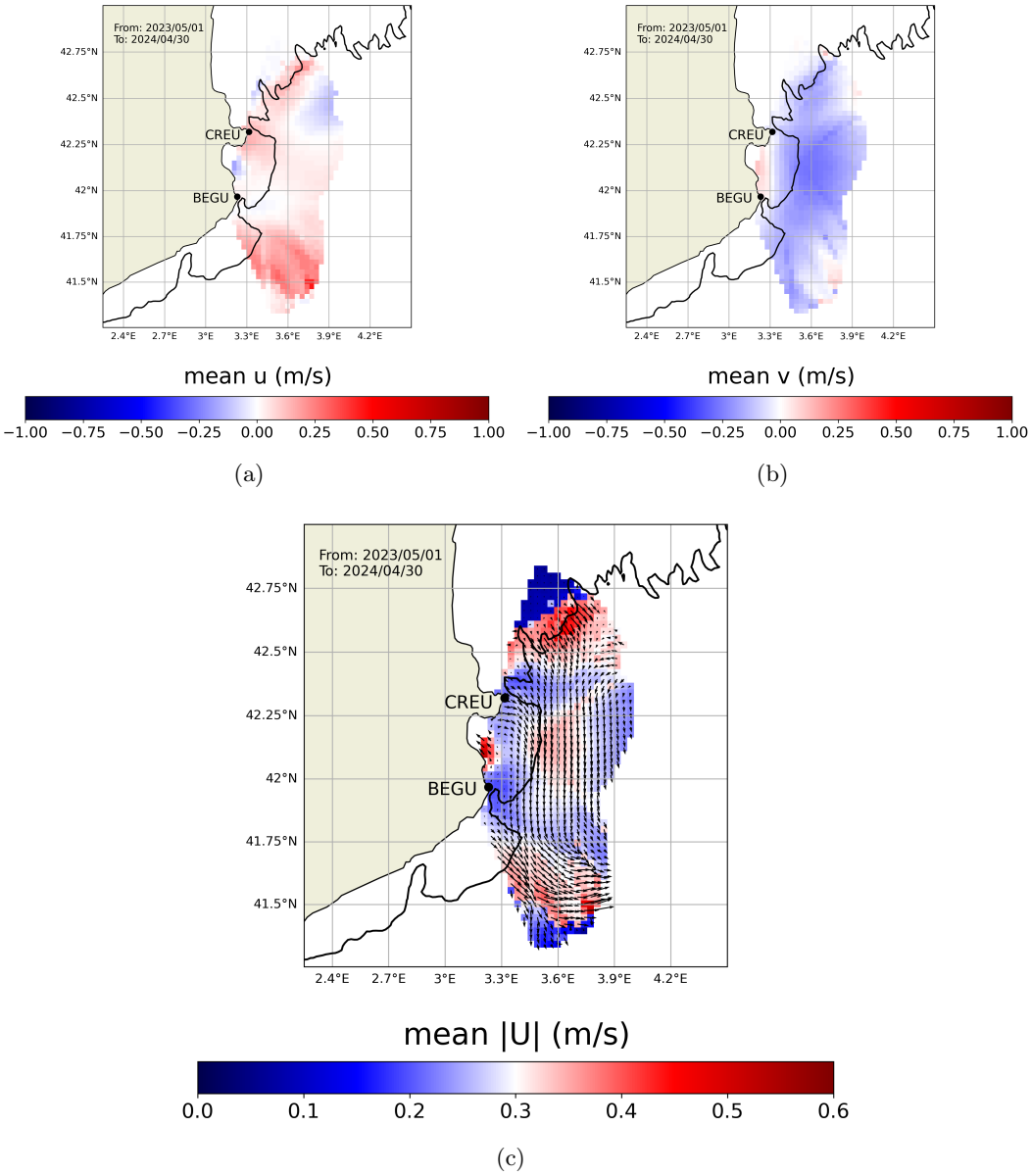

Figure 16: Spatial distribution of the 1^{st} statistical moment of total velocity vectors (U) derived from the ICATMAR HFR network and qualified as "*good data*" by the L3 QC model: (a) *mean* of total velocity u component, (b) *mean* of total velocity v component and (c) *mean* of the total velocity module $|U|$ (colour scale) and vector (black arrows). Calculation of the *mean* moments have been done for each cell of the grid used for total velocity estimations and over the time dimension for the 1-year period between May 1 of 2023 and April 30 of 2024. Black contour line offshore indicates the location of the 200 m depth isobath and black dots indicate the location of CREU and BEGU stations.

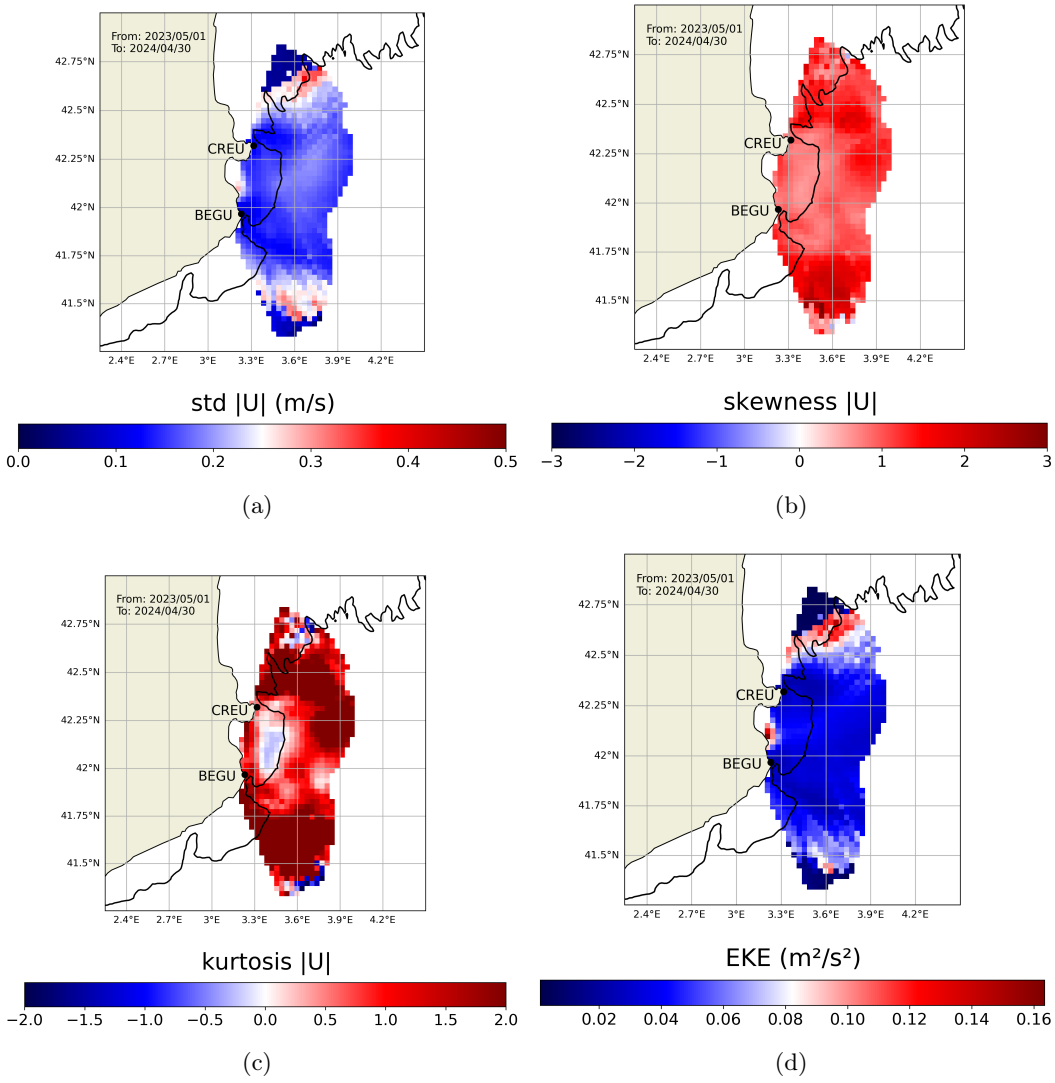

Figure 17: Spatial distribution of the 2^{nd} to 4^{th} statistical moments and the *EKE* estimated for the module of total velocity vectors ($|U|$) derived from the ICATMAR HFR network and qualified as "*good data*" by the L3 QC model: (a) *standard deviation (std)*, (b) *skewness*, (c) *kurtosis* (note that Fisher kurtosis has been used, where 0.0 is for a normal distribution) and (d) *EKE* as defined by Richardson [1983]. Calculation have been done for each cell of the grid used for total velocity estimations and over the time dimension for the 1-year period between May 1 of 2023 and April 30 of 2024. Black contour line offshore indicates the location of the 200 m depth isobath and black dots indicate the location of CREU and BEGU stations.

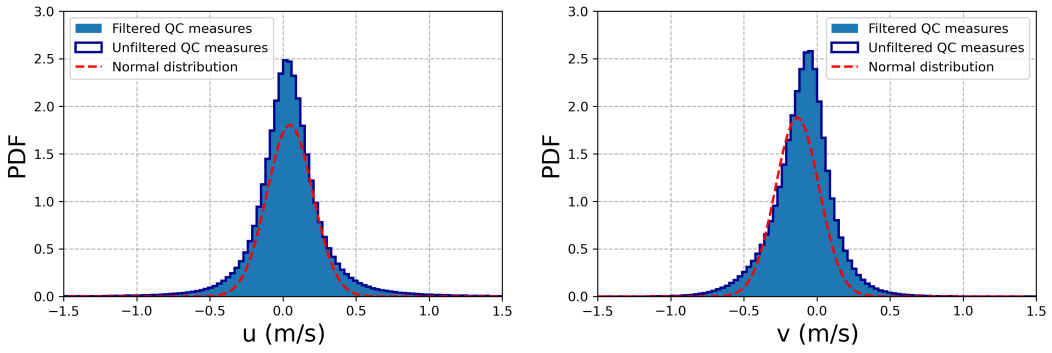

(a) (b)

Figure 18: Probability density functions (PDFs) of u (a) and v (b) components of total velocities derived from the ICATMAR HFR network. Blue filled bars and dark blue profiles correspond, respectively, to PDFs computed from total velocity vectors passing the QC assessment (thus, from only "*good data*") and to PDFs computed from all total velocity vectors before being evaluated by the complete QC assessment. Red dashed line depict the normal distribution associated to the "*good data*" dataset of each total velocity component.

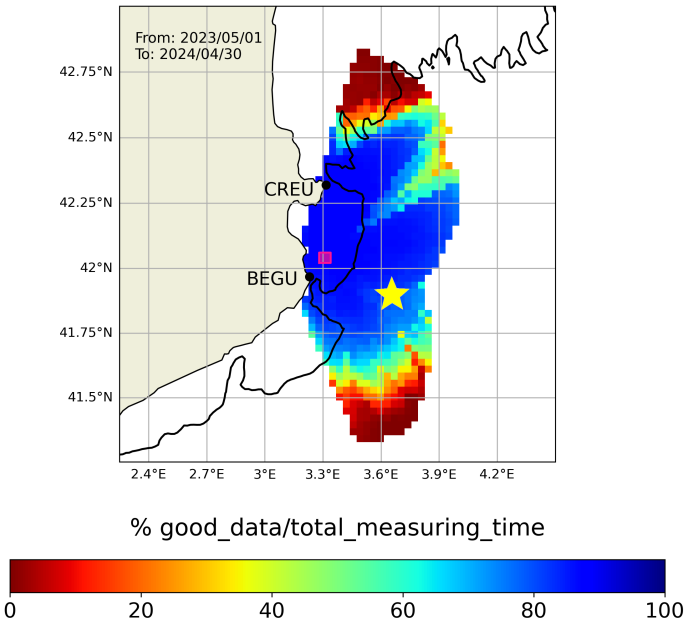

Figure 19: Map showing the location of Begur buoy (yellow star) and the experiment with drifting objects (i.e. bounding box indicated with a pink square), which have been used for the data validation of the 1^{st}-year sea surface current time-series derived from ICATMAR HFR. The percentage of good quality data over the analysed period is also shown in the background and is the same as the one shown in Figure 15a. Black contour line offshore indicates the location of the 200 m depth isobath and black dots indicate the location of CREU and BEGU stations.

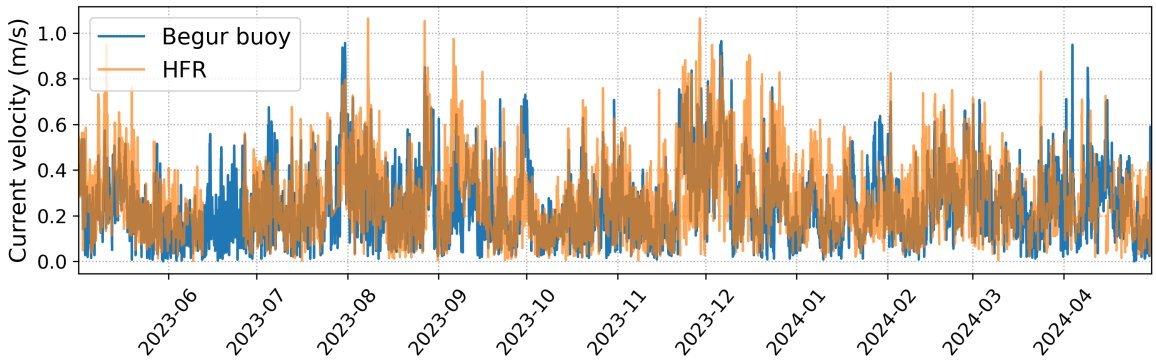

Figure 20: Time-series of sea surface current velocity module measured by the ICAT-MAR HFR network and Begur buoy, for the 1-year period analysed in this report (from 01/May/2023 to 30/April/2024). Data from HFR correspond to total velocities measured at the location of Begur buoy (41.92°N, 3.67°E).

quality was produced (Figure 19). The buoy is identified with the 2798 code and '*Cabo de Begur*' name in Puertos del Estado database. It is a Wavescan buoy model and uses a NORTEK Aquadopp Profiler, an acoustic Doppler current profiler, to obtain measures of marine currents. It collects data on current intensity and direction of propagation, with a reference point at 0°N and increasing clockwise. Data is collected for 10 minutes every hour to provide hourly time resolution. Data are collected at a depth of 3 m [Área de Medio Físico de Puertos del Estado, n.d.].

Figure 20 presents the current velocity module time-series of the HFR and the Begur buoy (measured at the same location, see Figure 19), where similar variability patterns can be observed. The PDFs of these time-series indicate that, as a general trend, current velocities measured by the HFR are slightly higher that those measured by the Begur buoy (Figure 21). Complementary, Figure 22 also shows the comparison between both time-series but adding the information of the current direction. It shows that most events with higher intensity currents were recorded around the same dates by both observing systems, with similar current directions (arrows orientations in the figure) the majority of the time.

2D histograms in Figure 23 show a more detailed picture of the relationship between both time series. Regarding the module of current velocities, the relationship plotted in Figure 23a shows that there is a positive correlation between the HFR and buoy measures. In particular, for velocity modules smaller than ∼0.3 m/s (which comprises more than 50% of the data, see the median in Figure 21), currents measured by the HFR tend to be slightly higher that those measured by the Begur buoy. This is in accordance with PDF distributions in Figure 21 and it could be related with the fact that surface currents are generally more intense than those found at greater depths. In this case, both compared observing systems are measuring the current at different depths: ∼1 m depth for the 13.5 MHz HFRs versus the 3 m depth of the buoy sensor.

An opposite relationship is observed in Figure 23 between current velocities measured by both observing systems. The 2D histogram suggests that, for velocity modules bigger than ∼0.5 m/s, HFR measures are slightly underestimated with respect the buoy measures. However, the low number of data above this threshold (see Figure 21) is not statistically significant and gathering more data will be required to obtain a more reliable interpretation on this.

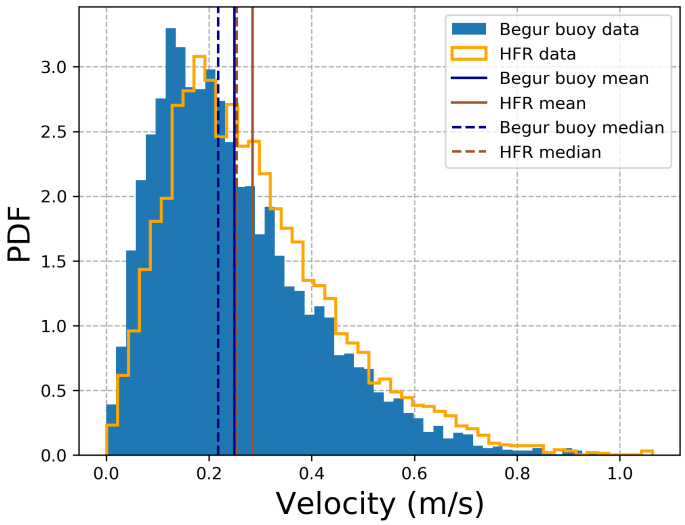

Figure 21: Probability density functions (PDFs) of sea surface current velocity module measured by the ICATMAR HFR network and Begur buoy, for the 1-year period analysed in this report (from 01/May/2023 to 30/April/2024). Data from HFR correspond to total velocities measured at the location of Begur buoy (41.92°N, 3.67°E). Mean and median are displayed for each PDF with solid and dashed vertical lines.

Regarding the 2D histogram in Figure 23b, HFR- and buoy-derived current directions show a positive correlation for angles between the range of 100°N and 250°N, while the correlation is not statistically significant for current directions with smaller and higher angles. This is in agreement with the mean current direction around the area of Begur buoy location, which is southward (see Figure 16c). Also, buoy data within this range is shown to be offset from the 1:1-relationship reference line, with the buoy measuring slightly greater current directions than those measured by the HFR. Again, this could be caused by the buoy measuring currents at 3 m depth, which would tend to be slightly advected to the right (compared with the ∼1 m depth measures representative of the 13.5 MHz HFRs), consistent with a classical Ekman layer theory where the velocity decays and turns clockwise with depth. Nonetheless, more data is needed to support this hypothesis.

Despite some discrepancies likely associated to differences in the measuring methods of the ICATMAR HFR and Begur buoy observing systems, both time series seem to roughly follow similar variation patterns of change in velocity and direction of the current, thus resulting in a successful exercise of data validation.

A second data validation exercise was performed using Lagrangian trajectories of drifting objects. On November 9th of 2023, a SAR exercise was organised within the ICATMAR HFR coverage area (see pink marker in Figure 19). A dummy configured vertically and a CODE buoy were released and recovered after 26 h, both following very close trajectories. The time series of HFR sea surface currents measured in November 9th 2023 were used to model Lagrangian trajectories (simulated with OpenDrift), which were compared with real trajectories of the dummy and CODE buoy (Figure 24).

Wind and Stokes drift effects were also added on the Lagrangian simulations, however such effects did not resulted in much difference in the drift trajectories (max. 800 m distance difference; see dotted and dashed green trajectories in Figure 24). Regarding the comparison

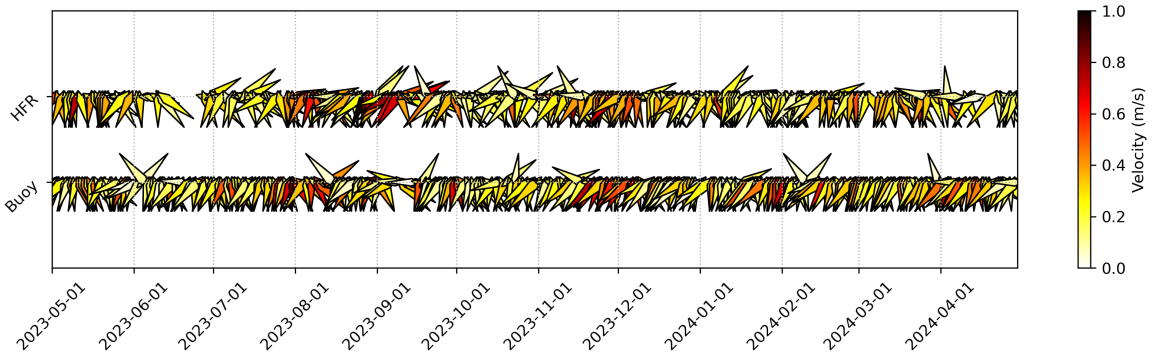

Figure 22: Sea surface current velocity (arrow's filling colour) and direction (arrow's orientation given as a clock-wise angle from the North) time-series measured by the ICATMAR HFR network and Begur buoy, for the 1-year period analysed in this report (from 01/May/2023 to 30/April/2024). Each arrow symbol displays the 24h-average of represented parameters. Data from HFR correspond to total velocities measured at the location of Begur buoy (41.92°N, 3.67°E).

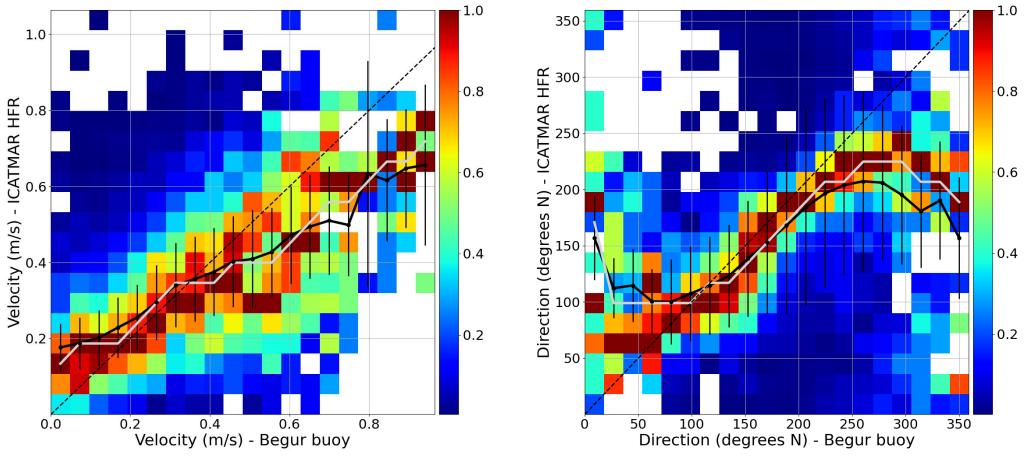

(a) (b)

Figure 23: 2D histograms showing the relationship between Begur buoy and ICATMAR HFR 1^{st}-year time-series of (a) sea surface current velocity and (b) direction. Data from HFR correspond to total velocities measured at the location of Begur buoy (41.92°N, 3.67°E). Colour scale indicates the number of counts of ICATMAR bins at each BEGUR bins normalized by the maximum. Black and grey lines display the mean and median, respectively; as a reference, the dashed black line shows the 1:1 correlation.

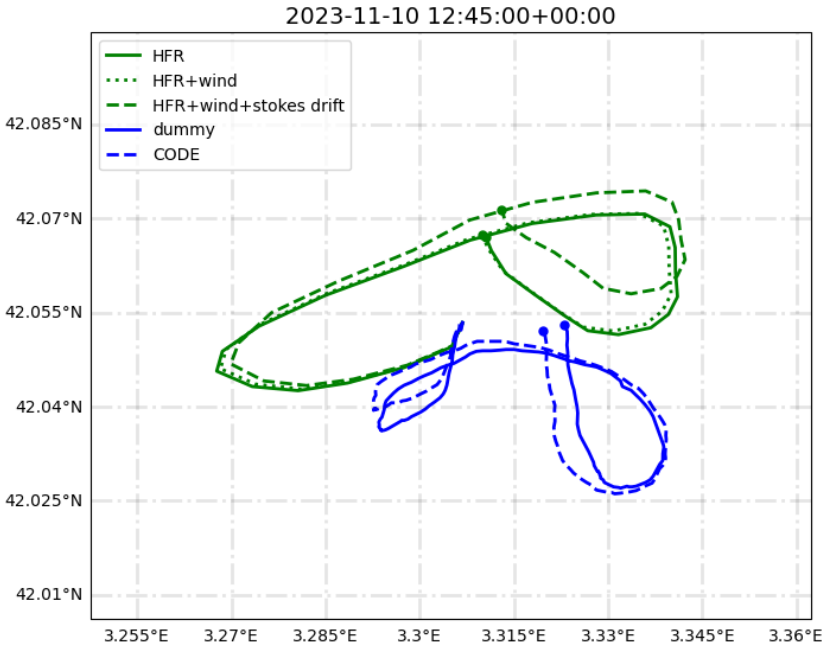

Figure 24: Trajectories of a dummy and a CODE buoy released during a SAR exercise performed on the 9^{th} November 2023. These are compared with Lagrangian trajectories simulated with OpenDrift based on ICATMAR HFR sea surface currents measured on the same date, both taking and not taking into account the effect of wind and stokes drift. Location of this SAR exercise is indicated in Figure 19 with a pink bounding box.

with real trajectories of the dummy and CODE buoy, the Lagrangian trajectories derived from the HFR were significantly close to them, with a separation between the real and simulated final positions of less than 2 km. The results of this second HFR data validation exercise are also important in order to test the assessment of HFR products for SAR operations [Quirós-Collazos et al., 2024a].

Further performance of drifting buoys exercises are planned by the ICATMAR Operational Oceanography team, which will contribute to validate the sea surface current results obtained by the ICATMAR HFR network.

5 Summary

The results of this report show that the deployment of the ICATMAR HFR network has been successful so far. During the 1^{st} year of operation, the HFR network provided good quality data on sea surface currents in the northern part of the Catalan sea for more than 90% of the time.

The evaluation of QC performance on radial velocities indicated that most of radial measures produced by CREU and BEGU stations were of good quality. While radial data coverage is high, a systematic lack of measures was detected in the outer crowns of both stations' coverage areas, as well as in a few particular bearings. After the L2 QC assessment, the effective range is around 80 km in both stations.

Regarding good quality radial measures, the majority of values were within the range $[-0.5, 0.5]$ m/s. Also, the average direction of radials is in accordance with the known predominant surface current in this region, the Liguro-Provençal-Catalan current, which flows roughly from north-east to south-west along the continental shelf.

For total velocity fields, the area with optimal coverage of good quality data falls within the range of latitudes $[41.6, 42.5]$ $^{\circ}N$. North and south of it, total velocity measures are not so often produced and, when produced, they tend to be discarded by the L3 QC assessment, specially through the *GDOP threshold* test.

Absolute values of good quality total velocities were majorly within the $[0.0, 0.8]$ m/s range, with an average value of ~ 0.3 m/s for the studied period. Similar to radials, the time average direction of the surface current field is also in accordance with the Liguro-Provençal-Catalan current.

As an exercise of data validation, HFR-derived currents were compared with those measured by the meteo-oceanic Begur buoy. Both showed similar variation patterns along the studied period, both in intensity and direction of the current. The observed discrepancies between them, though, were likely due to the fact that the buoy measures were taken at a slightly deeper depth (3 m) than those derived from the 13.5 MHz HFRs (∼1 m depth). As a second validation exercise, simulation of Lagrangian trajectories using HFR velocity fields were compared with real trajectories of two drifting objects that were released for 26 h in the coverage area of the ICATMAR HFR network. The obtained good results of this exercise were relevant to promote the use of HFR-derived data in save and rescue operations.

Future work will consist in the addition of the data to the time-series, together with the increase in data coverage provided by the antennas that have been installed later along the Catalan coast. This will help to reduce the uncertainty around some aspects discussed along the present report. Additionally, the results of this report will help adjust some of the QC parameters, such as the *Velocity threshold* or the *GDOP threshold*, to keep providing the best quality in sea surface currents for the Catalan sea region.

Appendix A

L2A, L2B and L3A examples

Listing A.1: Sample of a L2A radial file (.ruv) corresponding to the CREU antenna.

```
%CTF: 1.00
%FileType: LLUV rdls "RadialMap"
%LLUVSpec: 1.51 2021 07 01
%UUID: 3BD748FC—F383—43FC—8B3A—7213EB6570BE
%Manufacturer: CODAR Ocean Sensors. SeaSonde
%Site: CREU ""
%TimeStamp: 2023 02 17 11 00 00
%TimeZone: "UTC" +0.000 0 "UTC"
%TimeCoverage: 75.000 Minutes
%Origin: 42.3190500 3.3158500
%GreatCircle: "WGS84" 6378137.000 298.257223562997
%GeodVersion: "CGEO" 2.00 2019 03 05
%LLUVTrustData: all %% all lluv xyuv rbvd
%Suite: 101903199285177 21 04
```

```
%RangeStart: 2
%RangeEnd: 69
%RangeResolutionKMeters: 1.664243
%RangeCells: 68
%DopplerCells: 1024
%DopplerInterpolation: 2
%AntennaBearing: 96.0 True
%ReferenceBearing: 0 True
%AngularResolution: 5 Deg
%RiverBearing: 0.0 True
%PatternType: Measured
%PatternDate: 2022 03 04 18 06 37
%PatternResolution: 1.0 deg
%PatternUUID: D6DDC021—DAAD—47C0—9340—94EDD315177E
%AverSignalToNoise: 13.7
%AverDistanceToPattern: —1.6
%TransmitCenterFreqMHz: 13.500000
%TransmitBandwidthKHz: —90.068695
%TransmitSweepRateHz: 2.000000
%FirstOrderMethod: 0 2 70
%BraggSmoothingPoints: 2
%CurrentVelocityLimit: 150.0
%BraggHasSecondOrder: 1
%RadialBraggPeakDropOff: 100.000
%RadialBraggPeakNull: 10.000
%RadialBraggNoiseThreshold: 3.980
%RadialSplitBraggRatio: 6.310 0
%RadialDCBlock: 5.100 1
%PatternAmplitudeCorrections: 0.8315 0.6220
```

```
%PatternPhaseCorrections: —105.74 —84.46
%PatternAmplitudeCalculations: 2.4673 2.1575
%PatternPhaseCalculations: 142.49 —48.00
%RadialMusicParameters: 40.000 20.000 2.000
%FirstOrderCalc: 0
%MergeMethod: 1 MedianVectors
%MergedCount: 7
%TableType: LLUV RDL9
%TableColumns: 20
%TableColumnTypes: LOND LATD VELU VELV VFLG ESPC ETMP EDTP EASN MAXV MINV ERSC ERTC XDST YDST RNGE BEAR VELO HEAD SPRC
%TableRows: 990
%TableStart:
%%  Longitude Latitude U comp V comp VectorFlag Spatial Temporal Pattern SNR  Velocity Velocity Spatial Temporal X Distance Y Distance
    Range Bearing Velocity Direction Spectra
%%   (deg)    (deg)   (cm/s) (cm/s) (GridCode) Quality Quality Distance (dB)  Maximum  Minimum Count  Count   (km)     (km)    (km)  (True
    ) (cm/s)  (True)  RngCell
    3.3165550 42.3490104 0.106 6.053    0     6.197    4.174    0.0    10.2    3.670   —16.769   6      3     0.0581   3.3280  3.3285  1.0
          —6.054  181.0     2
    3.3366541 42.3447331 17.555 29.201   0     1.187    1.556    —7.4   12.8   —29.868 —35.628   1      2     1.7143   2.8531  3.3285  31.0
          —34.072  211.0     2
    3.3395921 42.3432897 21.591 29.701   0     1.807    7.915    —2.1   13.7   —16.769 —39.994   5      7     1.9564   2.6928  3.3285  36.0
          —36.719  216.0     2
    3.3423492 42.3416618 26.248 30.176   0     0.780    9.863    —4.0   12.3   —18.162 —39.994   2      7     2.1837   2.5121  3.3285  41.0
          —39.994  221.0     2
```

Listing A.2: Sample of a L2B radial file (.ruv) corresponding to the CREU antenna.

```
%CTF: 1.00
%FileType: LLUV rdls "RadialMap"
%LLUVSpec: 1.51 2021 07 01
%UUID: 94A2173D—76CE—4E7E—A4E6—6EAB650F560B
%Manufacturer: CODAR Ocean Sensors. SeaSonde
%Site: CREU ""
%TimeStamp: 2023 03 01 00 00 00
%TimeZone: "UTC" +0.000 0 "UTC"
%TimeCoverage: 75.000 Minutes
%Origin: 42.3190500 3.3158500
%GreatCircle: "WGS84" 6378137.000 298.257223562997
%GeodVersion: "CGEO" 2.00 2019 03 05
%LLUVTrustData: all all lluv xyuv rbvd
%Suite: 101903199285177 21 04
%RangeStart: 2
%RangeEnd: 69
%RangeResolutionKMeters: 1.664243
%RangeCells: 68
%DopplerCells: 1024
%DopplerInterpolation: 2
%AntennaBearing: 96.0 True
%ReferenceBearing: 0 True
%AngularResolution: 5 Deg
%RiverBearing: 0.0 True
%PatternType: Measured
%PatternDate: 2022 03 04 18 06 37
%PatternResolution: 1.0 deg
%PatternUUID: D6DDC021—DAAD—47C0—9340—94EDD315177E
```

```
%AverSignalToNoise: 20.7
%AverDistanceToPattern: —2.5
%TransmitCenterFreqMHz: 13.500000
%TransmitBandwidthKHz: —90.068695
%TransmitSweepRateHz: 2.000000
%FirstOrderMethod: 0 2 70
%BraggSmoothingPoints: 2
%CurrentVelocityLimit: 150.0
%BraggHasSecondOrder: 1
%RadialBraggPeakDropOff: 100.000
%RadialBraggPeakNull: 10.000
%RadialBraggNoiseThreshold: 3.980
%RadialSplitBraggRatio: 6.310 0
%RadialDCBlock: 5.100 1
%PatternAmplitudeCorrections: 0.8315 0.6220
%PatternPhaseCorrections: —105.74 —84.46
%PatternAmplitudeCalculations: 2.5923 1.4698
%PatternPhaseCalculations: —36.73 —143.45
%RadialMusicParameters: 40.000 20.000 2.000
%FirstOrderCalc: 0
%MergeMethod: 1 MedianVectors
%MergedCount: 7
%MergeMedianMethod: 1 balance
%MergeCloseness: 0.0001 km
%MergeMinimumVectors: 2
%MergeVectorLocation: False
%MergeSources: 7
%QCFileVersion: 2.0.0
%QCReference: Quality control reference: IOOS QARTOD HF Radar ver 2.0 June 2022
```

```
%QCFlagDefinitions: 1=pass 2=not_evaluated 3=suspect 4=fail 9=missing_data
%QCTestFormat: "test_name [qc_thresholds]: test_result"
%QCTest: qc_qartod_syntax (Q201) — Test applies to entire file. Thresholds=[N/A]: See results in column Q201
%QCTest: qc_qartod_valid_location (Q203) — Test applies to each row. Thresholds=[VFLG==128]: See results in column Q203 below
%QCTest: qc_qartod_maximum_velocity (Q202) — Test applies to each row. Thresholds=[ high_vel=140 (cm/s) max_vel=170 (cm/s) ]: See results in column Q202 below
%QCTest: qc_qartod_temporal_gradient (Q206) — Test applies to each row. Thresholds=[ gradient_temp_warn=30 (cm/s*hr) gradient_temp_fail=40 (cm/s*hr) ]: See results in column Q206 below
%QCTest: qc_qartod_spatial_median (Q205) — Test applies to each row. Thresholds=[ range_cell_limit=2.1 (range cells) angular_limit=10 (degrees) current_difference=30 (cm/s) ]: See results in column Q205 below
%QCTest: qc_qartod_avg_radial_bearing (Q207) — Test applies to entire file. Thresholds=[ reference_bearing=137 (degrees) warning=30 (degrees) failure=30 (degrees) ]: See result in column Q207 below
%QCTest: qc_qartod_radial_count (Q204) — Test applies to entire file. Thresholds=[ failure=50 (radials) warning_num=140 (radials) <valid_radials=885> ]: See results in column Q204 below
%QCTest: qc_qartod_primary_flag (PRIM) — Primary Flag — Highest flag value of Q201, Q203, Q202, Q206, Q205, Q207, Q204("not_evaluated" flag results ignored)
%TableType: LLUV RDL9
%TableColumns: 28
%TableColumnTypes: LOND LATD VELU VELV VFLG ESPC ETMP EDTP EASN MAXV MINV ERSC ERTC XDST YDST RNGE BEAR VELO HEAD SPRC Q201 Q203 Q202 Q206 Q205 Q207 Q204 PRIM
%TableRows: 885
%TableStart:
%% Longitude Latitude U comp V comp VectorFlag Spatial Temporal Pattern SNR Velocity Velocity Spatial Temporal X Distance Y Distance Range Bearing Velocity Direction Spectra Q201 Q203 Q202 Q206 Q205 Q207 Q204 PRIM
%%   (deg)    (deg) (cm/s) (cm/s) (GridCode) Quality Quality Distance (dB) Maximum Minimum Count Count (km) (km) (km) (True) (cm/s) (True) RngCell (flag) (flag) (flag) (flag) (flag) (flag) (flag) (flag)
  3.3165550 42.3490104 −0.221 −12.679 0 24.966 6.222 −3.5 22.7 47.334 −53.883 20    7    0.0581   3.328 3.3285  1.0  12.681  181.0    2
        1    1    1    1    1    1    1    1
  3.3200725 42.3488507 3.503 33.317  0 15.826  8.783    0.0 30.0 18.952 −53.883 16     4    0.3479  3.3103 3.3285  6.0 −33.501 186.0    2
```

```
       1    1    1    1    4    1    1    4
77  3.3235579 42.3484642 −5.311 −27.31 0 12.484 7.590  −5.7 22.1 36.418 −7.246  6     6   0.6351  3.2673 3.3285 11.0 27.821  191.0    2
       1    1    1    1    1    1    1    1
78  3.3269845 42.3478536 −5.007 −17.454 0 12.651 7.952 −3.8 23.4 36.418 −44.361 30    7   0.9175  3.1996 3.3285 16.0 18.158  196.0    2
       1    1    1    1    1    1    1    1
79  3.3303262 42.3470238 16.188 42.149 0  3.608  8.438   0.0 31.1 −25.502 −49.517 1     5   1.1928  3.1074 3.3285 21.0 −45.151 201.0    2
       1    1    1    1    4    1    1    4
80  3.3335577 42.3459810 −2.567 −5.26 0 6.627 11.640   −6.5 22.4 25.502 −47.334 1     7   1.4591  2.9916 3.3285 26.0  5.853  206.0    2
       1    1    1    1    1    1    1    1
81  3.3366541 42.3447331 21.014 34.954 0  5.917 19.927   0.0 35.7  1.487 −40.784  1     3   1.7143  2.8531 3.3285 31.0 −40.784 211.0    2
       1    1    1    3    1    1    1    3
82  3.3395921 42.3432897 −38.424 −52.854 0 4.366 8.187  0.0 20.3 73.532 49.517   4     2   1.9564  2.6928 3.3285 36.0 65.345  216.0    2
       1    1    1    4    4    1    1    4
83  3.3423492 42.3416618 −35.721 −41.067 0 21.832 21.286 0.0 17.4 75.715 33.143  2     2   2.1837  2.5121 3.3285 41.0 54.429  221.0    2
       1    1    1    4    4    1    1    4
84  3.3449043 42.3398617 23.565 22.741 0  0.000 18.952   −7.4 29.5 −13.796 −51.7 1     2   2.3943  2.3122 3.3285 46.0 −32.748 226.0    2
       1    1    1    2    1    1    1    1
85  3.3557328 42.3237306 −7.157 −1.13 0 0.958  3.214   −5.7 36.4 13.796 5.063   3     3   3.2875  0.5207 3.3285 81.0  7.246  261.0    2
       1    1    1    2    1    1    1    1
86  3.3562205 42.3185199 2.578 −0.046 0  5.640 14.155   −3.6 41.5 9.429 −34.235  1     6    3.328  −0.0581 3.3285 91.0 −2.579 271.0    2
       1    1    1    1    1    1    1    1
87  3.3485065 42.3014323 5.175 −3.763 0  3.820  6.004   0.0 39.9  7.246 −12.403  1     2   2.6928  −1.9564 3.3285 126.0 −6.399 306.0   2
       1    1    1    2    1    1    1    1
88  3.3463134 42.2993871 −8.762 7.622 0  2.953 10.700   0.0 31.0 15.979 −12.403  2     5   2.5121  −2.1837 3.3285 131.0 11.613 311.0    2
       1    1    1    1    1    1    1    1
89  3.3438886 42.2974915 −5.032 5.214 0  3.471  8.130   0.0 35.0 13.796 −10.219  4     5   2.3122  −2.3943 3.3285 136.0 7.247  316.0    2
       1    1    1    1    1    1    1    1
90  3.3412507 42.2957599 0.935 −1.156 0  2.208  5.330   0.0 39.3  3.971 −21.135  1     5   2.0947  −2.5867 3.3285 141.0 −1.487 321.0   2
       1    1    1    1    1    1    1    1
```

```
91  3.3384196 42.2942056 2.2 −3.263  0  4.109  5.503   0.0 32.3 11.613 −18.952 18    6   1.8613  −2.7595 3.3285 146.0 −3.936 326.0  2
        1    1    1    1    1    1    1    1
92  3.3354170 42.2928403 3.894 −7.029 0  6.600 12.139   0.0 38.7 11.613 −42.967  1    6   1.6137  −2.9112 3.3285 151.0 −8.036 331.0  2
        1    1    1    1    1    1    1    1
93  3.3322657 42.2916743 6.818 −15.321 0 0.843  6.550   0.0 38.1 −8.036 −23.319 1     2   1.3538  −3.0407 3.3285 156.0 −16.769 336.0 2
        1    1    1    1    1    1    1    1
94  3.3289896 42.2907167 5.812 −16.888 0 6.729 13.553   0.0 37.8 −5.063 −53.883 2     3   1.0837  −3.1472 3.3285 161.0 −17.861 341.0 2
        1    1    1    1    1    1    1    1
95  3.3256136 42.2899746 6.167 −24.745 0 6.144 12.286   0.0 36.5  −2.88 −51.7   4     4   0.8052  −3.2296 3.3285 166.0 −25.502 346.0 2
        1    1    1    1    1    1    1    1
96  3.3221634 42.2894536 5.125 −32.376 0 2.497 10.163   0.0 34.5 −21.135 −49.517 6     5   0.5207  −3.2875 3.3285 171.0 −32.779 351.0 2
        1    1    1    1    1    1    1    1
97  3.3186652 42.2891579 2.529 −36.184 0 6.534  7.019   0.0 36.0 −5.063 −49.517 10    6   0.2322  −3.3204 3.3285 176.0 −36.272 356.0 2
        1    1    1    1    1    1    1    1
98  3.3151457 42.2890895 −0.597 −34.23 0 2.013 8.147   0.0 40.5 −20.345 −49.517 1    3   −0.0581 −3.328 3.3285 181.0 −34.235 1.0    2
        1    1    1    1    1    1    1    1
99  3.2962667 42.3452563 31.076 −56.031 0 4.390 7.597  −4.8 22.5 82.265 53.883  18    7   −1.6137 2.9112 3.3285 331.0 64.072  151.0   2
        1    1    1    1    1    1    1    1
100 3.3060774 42.3481244 10.07 −40.37 0 18.311 6.703   −4.1 23.4 82.265 −25.502 22    7   −0.8052 3.2296 3.3285 346.0 41.607  166.0   2
        1    1    1    1    4    1    1    4
101 3.3095307 42.3486459 −1.141 7.203 0  9.316  9.754   0.0 38.8 56.067 −32.051  5     6   −0.5207 3.2875 3.3285 351.0 −7.293 171.0   2
        1    1    1    1    1    1    1    1
102 3.3130321 42.3489419 −0.256 3.661 0  8.827  7.244   0.0 36.3 47.334 −23.319 12    7   −0.2322 3.3204 3.3285 356.0 −3.67  176.0   2
        1    1    1    1    1    1    1    1
103 3.3169078 42.3639901 −0.188 −10.775 0 21.783 10.025 −4.1 29.4 45.151 −60.433 15   7   0.0871  4.9919 4.9927  1.0  10.777  181.0   3
        1    1    1    1    1    1    1    1
104 3.3221852 42.3637505 1.676 15.938  0  9.004  8.347   0.0 35.2 25.502 −56.067 11    7   0.5219  4.9653 4.9927  6.0 −16.026 186.0   3
        1    1    1    1    1    1    1    1
105 3.3274144 42.3631705 −2.785 −14.318 0 10.895 7.628 −3.6 28.6 32.051 −23.319 9     7   0.9527   4.901 4.9927  11.0 14.586  191.0   3
```

```
         1    1    1    1    1    1    1    1
106   3.3325554 42.3622545 −4.372 −15.237 0 12.240 4.524 −3.4 30.2 32.051 −29.868 10    7   1.3762  4.7993 4.9927 16.0 15.852  196.0    3
         1    1    1    1    1    1    1    1
107   3.3375689 42.3610095 7.188 18.711  0  5.170 10.980    0.0 42.0 −5.853 −58.25  2     5   1.7892  4.6611 4.9927 21.0 −20.044 201.0    3
         1    1    1    1    1    1    1    1
108   3.3424169 42.3594450 −1.915 −3.924 0 11.744 11.689 −3.0 34.0 27.685 −49.517 4     7   2.1887  4.4874 4.9927 26.0  4.366   206.0    3
         1    1    1    1    1    1    1    1
109   3.3470622 42.3575728 7.313 12.161  0  6.806 13.848   −3.2 34.0 4.761 −29.078  3     3   2.5714  4.2796 4.9927 31.0 −14.191 211.0    3
         1    1    1    1    1    1    1    1
110   3.3514696 42.3554073 8.114 11.158  0  5.303 14.261   −7.1 23.5  3.67 −31.261  1     3   2.9346  4.0392 4.9927 36.0 −13.796 216.0    3
         1    1    1    4    1    1    1    4
111   3.3556055 42.3529650 24.622 28.297 0 7.955  7.641    0.0 35.1 −29.868 −45.151 1     2   3.2755   3.768 4.9927  41.0 −37.51  221.0    3
         1    1    1    2    1    1    1    1
112   ..............................................................
113   ..............................................................
114   ..............................................................
115   ..............................................................
116   ..............................................................
117
118   3.1186675 42.9003480 0.437 −1.734 0  5.729  4.207   −3.2 7.8 10.219 −0.697   1     4  −16.1047 64.5923 66.5697 346.0 1.788 165.9   40
          1    1    1    1    1    1    1    1
119   3.1883240 42.9108684 −5.234 32.727 0 10.568 9.824   0.0  7.8 −23.319 −42.967 2     2  −10.4138 65.7501 66.5697 351.0 −33.143 170.9
      40   1    1    1    2    4    1    1    4
120   3.6999326 42.8974254 −2.24 −4.54 0  0.000  4.366   −3.2 6.5  9.429  0.697    1     2   31.3709 64.3199 71.5625 26.0 5.063   206.3   43
         1    1    1    2    1    1    1    1
121   3.1037297 42.9439298 0.17 −0.676  0  0.000  0.000   −6.7 9.8  0.697  0.697    1     2  −17.3125 69.4368 71.5625 346.0 0.697 165.9   43
         1    1    1    2    1    1    1    1
122 %TableEnd:
123 %%
```

```
%TableType: rads rad1
%TableColumns: 31
%TableColumnTypes: TIME AMP1 AMP2 PH13 PH23 CPH1 CPH2 SNF1 SNF2 SNF3 SSN1 SSN2 SSN3 DGRC DOPV DDAP RADV RAPR RARC RADR RMCV RACV RABA RTYP STYP TYRS TMON TDAY THRS TMIN TSEC
%TableRows: 7
%TableStart: 2
%%  Time    Calculated  Calculated Corrected    Noise Floor SignalToNoise Diag Valid Dual Radial RadsV Rads Max Vel Vel Bearing Radial Spectra Time
%% FromStart Amp1 Amp2 Phase13 Phase23 Phase1 Phase2 NF1 NF2 NF3 SN1 SN2 SN3 Range Dopplr Angle Vector per Range Range Max Aver Average Type Type Year Mo Dy Hr Mn S
%% Seconds (1/v^2) (1/v^2) (deg) (deg) (deg) (deg) (dBm) (dBm) (dBm) (dB) (dB) (dB) Cell Cells Prcnt Count Range Cells (km) (cm/s) (cm/s) (deg CWN)
% -1800 2.5556 1.3747 -36.4 -171.4 -105.7 -84.5 -139.0 -139.0 -133.0 44.0 44.0 46.0 3 2673 34 1122 27 68 63.2 -86.6 25.8 47.3 2 0 2023 2 28 23 30 0
% -1200 2.2970 1.5476 -37.9 -170.4 -105.7 -84.5 -139.0 -139.0 -133.0 43.0 45.0 46.0 3 2701 34 1067 27 68 63.2 82.3 27.4 52.2 2 0 2023 2 28 23 40 0
% -600 2.5923 1.4698 -36.7 -143.5 -105.7 -84.5 -139.0 -138.0 -133.0 46.0 43.0 47.0 3 2686 36 1050 26 68 63.2 -75.7 27.7 41.4 2 0 2023 2 28 23 50 0
%    0 2.3484 1.6229 -37.8 -164.6 -105.7 -84.5 -139.0 -138.0 -132.0 44.0 45.0 45.0 3 2646 40 1129 28 68 63.2 80.1 27.7 45.4 2 0 2023 3 1 0 0 0
%  600 2.2579 1.5286 -38.6 -146.1 -105.7 -84.5 -139.0 -139.0 -133.0 46.0 45.0 46.0 4 2655 38 1080 28 68 64.9 -77.9 28.1 47.6 2 0 2023 3 1 0 10 0
% 1200 2.6604 1.6233 -37.3 -143.2 -105.7 -84.5 -139.0 -139.0 -132.0 48.0 46.0 46.0 5 2673 34 1031 26 68 63.2 -77.9 26.0 42.0 2 0 2023 3 1 0 20 0
% 1800 2.7228 1.8302 -36.1 -140.5 -105.7 -84.5 -139.0 -139.0 -132.0 47.0 45.0 48.0 4 2764 32 913 22 68 69.9 -77.9 27.6 42.6 2 0 2023 3 1 0 30 0
%TableEnd: 2
%%
%TableType: rcvr rcv3
```

```
%TableColumns: 33
%TableColumnTypes: TIME RTMP MTMP XTRP RUNT SP24 SP05 SN05 SP12 XPHT XAHT XAFW XARW X1VR XP28 XP05 GRMD GDMD GSLK GSUL PLLL HTMP HUMI RBIA EXTA EXTB CRUN TYRS TMON TDAY THRS TMIN TSEC
%TableRows: 15
%TableStart: 3
%%  Minutes Rcvr Awg XmitTrip AwgRun Supply +5VDC —5VDC +12VDC XInt XAmp XForw XRefl Xmit X+Ampl X+5V GpsRcv GpsDsp GpsSat GpsSat PLL HiRcvr Humid Supply Extern Extern CompRunTime Date
%% FromStart degC degC HexCode Seconds Volts Volts Volts Volts degC degC Watts Watts VSWR Volts Volts Mode Mode Lock Unlock Unlock degC % Amps InputA InputB Minutes Year Mo Dy Hr Mn Sec
% —35.0 30 40 0 200649 0.0 5.1 —5.00 11.95 27 31 37 2 1.4 24.37 5.05 0 0 11 0 0 29.2 27 0.0 0 0 924.50 2023 2 28 23 25 0
% —30.0 30 40 0 200949 0.0 5.1 —5.00 11.95 27 31 37 2 1.4 24.37 5.05 0 0 11 0 0 29.4 27 0.0 0 0 929.51 2023 2 28 23 30 0
% —25.0 30 40 0 201248 0.0 5.1 —5.00 12.02 27 31 37 1 1.4 24.37 5.05 0 0 11 0 0 29.4 27 0.0 0 0 934.77 2023 2 28 23 35 0
% —20.0 30 40 0 201547 0.0 5.1 —5.00 11.95 27 31 37 2 1.4 24.37 5.05 0 0 11 0 0 29.5 27 0.0 0 0 939.54 2023 2 28 23 40 0
% —15.0 30 39 0 201847 0.0 5.1 —5.00 12.02 27 31 38 1 1.4 24.37 5.05 0 0 11 0 0 29.2 27 0.0 0 0 944.59 2023 2 28 23 45 0
% —10.0 30 40 0 202146 0.0 5.1 —5.00 11.95 27 31 37 1 1.5 24.37 5.05 0 0 11 0 0 29.3 27 0.0 0 0 949.56 2023 2 28 23 50 0
% —5.0 30 40 0 202445 0.0 5.1 —5.00 11.95 27 31 37 2 1.4 24.37 5.05 0 0 11 0 0 29.5 27 0.0 0 0 954.57 2023 2 28 23 55 0
%  0.0 30 40 0 202744 0.0 5.1 —5.00 11.95 27 31 38 2 1.4 24.37 5.05 0 0 10 0 0 29.3 27 0.0 0 0 959.57 2023 3 1 0 0 0
%  5.0 30 40 0 203044 0.0 5.1 —5.00 12.02 27 31 38 2 1.4 24.37 5.05 0 0 11 0 0 29.5 27 0.0 0 0 964.76 2023 3 1 0 5 0
% 10.0 30 40 0 203344 0.0 5.1 —4.98 11.80 27 31 38 1 1.4 24.37 5.05 0 0 10 1 0 29.3 27 0.0 0 0 969.60 2023 3 1 0 10 0
% 15.0 30 40 0 203643 0.0 5.1 —5.00 12.02 27 31 37 2 1.4 24.37 5.05 0 0 11 0 0 29.5 27 0.0 0 0 974.60 2023 3 1 0 15 0
% 20.0 30 40 0 203942 0.0 5.1 —5.00 11.95 27 32 37 1 1.4 24.37 5.05 0 0 10 1 0 29.2 27 0.0 0 0 979.62 2023 3 1 0 20 0
% 25.0 30 40 0 204241 0.0 5.1 —5.00 11.95 27 31 38 2 1.5 24.37 5.05 0 0 12 0 0 29.5 27 0.0 0 0 984.62 2023 3 1 0 25 0
% 30.0 30 40 0 204541 0.0 5.1 —5.00 11.95 27 32 38 2 1.4 24.37 5.05 0 0 12 0 0 29.5 27 0.0 0 0 989.63 2023 3 1 0 30 0
% 35.0 30 40 0 204840 0.0 5.1 —4.98 12.02 27 31 38 2 1.5 24.37 5.05 0 0 12 0 0 29.3 27 0.0 0 0 994.64 2023 3 1 0 35 0
%TableEnd: 3
%%
%ProcessedTimeStamp: 2023 03 01 00 40 19
%ProcessingTool: "LLUVMusic" 13.4.2
%ProcessingTool: "LLUVMerger" 3.2.1
```

```
%ProcessingTool: "LLUVCutoff" 3.1.0
%ProcessingTool: "LLUVArchiver" 1.0.0
%End:
```

Listing A.3: Sample of a L3A total velocities file (.tuv).

```
%CTF: 1.00
%FileType: LLUV tots "CurrentMap"
%LLUVSpec: merge_radials 0.5 2025 03 13
%UUID: edda2e11—f692—473c—8e5f—856754f27753
%Manufacturer: CODAR Ocean Sensors. SeaSonde
%Site: CATS ""
%TimeStamp: 2025 02 11 06 00 00
%TimeZone: "UTC" +0.000 0 "UTC"
%TimeCoverage: 75.000 Minutes
%Origin: 40.5061167  1.1244500
%GreatCircle: "WGS84" 6378137.000 298.257223562997
%DistanceMethod: "haversine" 1.0 2023 02 27 defined in merge_radials 0.5
%LLUVTrustData: all %% all lluv xyuv rbvd
%GridAxisOrientation: 0.0 True
%GridFileName: "hfradar_totals_grid_icatmar.nc"
%GridVersion: 1.0
%GridTimeStamp: 2024 03 07 15 45 03
%GridLastModified: 2024 03 07 15 45 03
%GridAxisOrientation: 0.0 DegNCW
%GridSpacing: 3.000 km
%AveragingRadius: 6100.0 km
%DistanceAngularLimit: None
%CurrentVelocityLimit: None
%TableType: LLUV TOT4
%TableColumns: 18
%TableColumnTypes: LOND LATD VELU VELV VFLG VELO HEAD UQAL VQAL CQAL GDOP S1CN S2CN S3CN S4CN S5CN S6CN S7CN
%TableRows: 2203
%TableStart:
```

```
%%  Longitude Latitude U comp V comp VectorFlag Velocity Direction Std_U Std_V COV GDOP Site Contri Site Contri Site Contri Site Contri
    Site Contri Site Contri Site Contri
%%   (deg)    (deg)   (cm/s) (cm/s) (GridCode) (cm/s) (True) (cm/s) (cm/s) (cm2/s2) (unitless) #1     #2        #3        #4        #5
           #6        #7
    1.7244999 40.5031013 47.217 3.780    0   47.368  85.4    9.645  1.639 −7.175  2.801   0     0     0     0     0     10     1
    1.7598400 40.5031013 77.644 2.013    0   77.670  88.5    9.826  1.631 −7.046  3.074   0     0     0     0     0     9      1
    1.6184800 40.5301018 62.011 −5.966   0   62.297  95.5   26.356  8.165 −201.991 2.832 0     0     0     0     0     5      1
    1.6538200 40.5301018 63.127 −7.618   0   63.585  96.9   24.596  6.825 −159.555 2.802 0     0     0     0     0     10     1
    1.6891600 40.5301018 55.220 −7.296   0   55.700  97.5   10.327  2.052 −1.451  2.335   0     0     0     0     0     6      2
    1.7244999 40.5301018 67.931 −3.187   0   68.006  92.7    7.110  1.287  4.378  1.711   0     0     0     0     0     10     4
    1.7598400 40.5301018 73.693 −1.197   0   73.702  90.9    5.956  1.020  1.281  1.831   0     0     0     0     0     12     3
    1.7951800 40.5301018 88.376 3.500    0   88.445  87.7    4.496  1.167  4.990  1.529   0     0     0     0     0     7      6
    1.6184800 40.5570984 60.834 −6.609   0   61.192  96.2    7.009  0.734  3.536  2.110   0     0     0     0     0     6      2
    1.6538200 40.5570984 60.602 −7.028   0   61.008  96.6    6.074  0.661  2.420  2.099   0     0     0     0     0     10     2
    1.6891600 40.5570984 63.839 −6.772   0   64.197  96.1    6.953  0.783  4.232  1.414   0     0     0     0     0     10     5
    1.7244999 40.5570984 58.197 −4.209   0   58.349  94.1    7.327  0.818  4.803  1.506   0     0     0     0     0     9      6
    1.7598400 40.5570984 58.547 −3.202   0   58.634  93.1    7.122  1.293  4.995  1.305   0     0     0     0     0     12     6
    1.7951800 40.5570984 69.096 −0.424   0   69.097  90.4    7.318  1.891 13.591  1.380   0     0     0     0     0     7      9
    1.8305200 40.5570984 65.458 1.008    0   65.466  89.1    8.418  2.221 18.439  1.430   0     0     0     0     0     10     6
    1.8658600 40.5570984 67.202 4.792    0   67.372  85.9   18.146  4.822 87.236  1.664   0     0     0     0     0     5      8
    1.9012001 40.5570984 68.870 12.560   0   70.005  79.7   14.783  3.920 57.697  1.768   0     0     0     0     0     8      4
    1.9365400 40.5570984 49.957 12.598   0   51.521  75.8    8.486  3.676 29.778  1.810   0     0     0     0     0     8      3
    1.9718800 40.5570984 82.476 23.849   0   85.855  73.9    8.778  3.810 31.965  2.807   0     0     0     0     0     8      1
    2.0072200 40.5570984 67.833 23.585   0   71.816  70.8    8.889  3.991 34.171  2.018   0     0     0     0     0     9      2
    2.0425601 40.5570984 56.756 19.615   0   60.050  70.9   11.260  5.141 56.573  2.334   0     0     0     0     0     6      2
    1.6184800 40.5840988 52.687 −6.066   0   53.035  96.6    3.827  0.543  0.636  1.838   0     0     0     0     0     10     2
    1.6538200 40.5840988 60.621 −7.104   0   61.035  96.7    5.738  0.642  2.105  2.063   0     0     0     0     0     11     2
  ..............................................................
  ..............................................................
```

```
  ..............................................................
  ..............................................................
  ..............................................................

    3.5621800 42.7980995 77.845 -11.825 0   78.738  98.6   85.925 26.356 -2263.843 12.419 6   6    0    0    0    0    0
    3.5975201 42.7980995 192.795 -51.244 0 199.489 104.9  466.010 144.599 -67383.809 15.749 1  6    0    0    0    0    0
    3.5268400 42.8250999 84.379 -13.744 0   85.491  99.3   85.361 26.164 -2232.537 12.205 7   4    0    0    0    0    0
    3.5621800 42.8250999 8.141 7.609    0   11.144  46.9   39.079 12.185 -475.721 9.443 7    6    0    0    0    0    0
%TableEnd:
%%
%TableType: MRGS src3
%TableColumns: 15
%TableColumnTypes: SNDX SITE OLAT OLON COVH RNGS PATK REFB NUMV MAXN MAXS MAXE MAXW PATH UUID
%TableRows: 7
%TableStart: 2
%% Site  Site     Origin    Origin   Coverage RangeStep Pattern Reference Vectors Maximum Maximum   Maximum   Maximum
                                  Source                                          UUID
%% Index          Latitude  Longitude (minutes) (km)    Kind  Bearing           North     South     East      West
                                    Path
%%
%    1  "CREU"   42.3190500 3.3158500   75.000  1.664243 "Meas"  126.0    900    43.0387649 41.5336781 4.2728898 3.0837803          "/home/
    lquiros/data/radar/L2B/CREU/2025/02/RDLm_CREU_2025_02_11_0600_l2b.ruv" "EECE5F8F-6420-40B0-A29F-3CFD22FAA00B"
%    2  "BEGU"   41.9671667 3.2305333   75.000  1.664243 "Meas"  132.0   1169    42.8691941 41.2239339 4.3488886 3.2115397          "/home/
    lquiros/data/radar/L2B/BEGU/2025/02/RDLm_BEGU_2025_02_11_0600_l2b.ruv" "A5DF37A5-24BF-494D-B2D9-8A4ACB8E6DEE"
%    3  "TOSS"   41.7157000 2.9339000   75.000  1.664243 "Idea"  194.0   1849    42.4703825 40.8226135 3.7170169 1.9277334          "/home/
    lquiros/data/radar/L2B/TOSS/2025/02/RDLi_TOSS_2025_02_11_0600_l2b.ruv" "7228D888-C0EB-423C-805B-E919FCBF1B71"
%    4  "AREN"   41.5775833 2.5577333   75.000  1.664243 "Meas"  199.0   1433    41.7741919 40.6935683 3.6770701 1.6770235          "/home/
    lquiros/data/radar/L2B/AREN/2025/02/RDLm_AREN_2025_02_11_0600_l2b.ruv" "AC51BD1D-DD02-4C95-B22B-78BC5262B287"
%    5  "PBCN"   41.3475833 2.1740500   75.000  1.664243 "Meas"  177.0   1210    42.0948726 40.5992996 3.2072712 1.2505906          "/home/
```

```
    lquiros/data/radar/L2B/PBCN/2025/02/RDLm_PBCN_2025_02_11_0600_l2b.ruv" "631EEC38—DB1A—45A8—B4F3—3935E147AA1E"
%    6  "GNST"  41.2560667 1.9221833  75.000  1.664243 "Meas"  208.0   1500    41.3513952 40.4173372 3.0213736 0.9690486          "/home/
    lquiros/data/radar/L2B/GNST/2025/02/RDLm_GNST_2025_02_11_0600_l2b.ruv" "2A8D9C91—BC4A—422A—907A—8D2FB66642C2"
%    7  "SCAL"  41.1862833 1.6073000  75.000  1.664243 "Idea"  217.0    573    41.8605880 40.5102621 2.4465402 1.2521100          "/home/
    lquiros/data/radar/L2B/SCAL/2025/02/RDLi_SCAL_2025_02_11_0600_l2b.ruv" "027AD9B1—041A—481C—B98A—9B9757560672"
%TableEnd: 2
%%
%%
%ProcessedTimeStamp: 2025 03 26 18 17 03
%ProcessingTool: merge_radials 0.5
%End:
```

Bibliography

A. Castellón, J. Font, and E. García-Ladona. The Liguro-Provençal-Catalan current (NW Mediterranean) observed by Doppler profiling in the Balearic Sea. Scientia Marina, 54(3): 269–276, 1990.

L. Corgnati, C. Mantovani, A. Novellino, A. Rubio, and J. Mader. Recommendation Report 2 on improved common procedures for HFR QC analysis. Technical report, Joint European Research Infrastructure network for Coastal Observatory - Novel European eXpertise for coastal observaTories - JERICO-NEXT. WP5-Data Management, Deliberable 5.14, Version 1.0., 2018.

E.U. Copernicus Marine Service Information (CMEMS). Mediterranean sea physics analysis and forecast. Marine Data Store (MDS), 2019. doi: 10.48670/mds-00359. Product: "MEDSEA_ANALYSISFORECAST_PHY_006_013" (Accessed on 08/Mar/2023).

IOC-UNESCO. Ocean data standards, vol. 3: Recommendation for a quality flag scheme for the exchange of oceanographic and marine meteorological data. Paris. Intergovernmental Oceanographic Commission of UNESCO, IOC Manuals and Guides, 54, Vol. 3:12 pp. (English.)(IOC/2013/MG/54–3), 2013.

M. Juza, B. Mourre, L. Renault, S. Gómara, K. Sebastián, S. Lora, J. P. Beltran, B. Frontera, B. Garau, C. Troupin, M. Torner, E. Heslop, B. Casas, R. Escudier, G. Vizoso, and J. Tintoré. Socib operational ocean forecasting system and multi-platform validation in the western mediterranean sea. Journal of Operational Oceanography, 9(sup1), 2016. doi: 10.1080/1755876X.2015.1117764. Product: "WMOPv2.2r ROMS Forecast (with data assimilation)" (Accessed on 27/Feb/2023).

Yeping Lai, Hao Zhou, Yuming Zeng, and Biyang Wen. Quantifying and reducing the doa estimation error resulting from antenna pattern deviation for direction-finding hf radar. Remote Sensing, 9(12), 2017. doi: 10.3390/rs9121285.

B. Lipa, B. Nyden, D. Ullman, and E. Terrill. Seasonde radial velocities: Derivation and internal consistency. Journal of Oceanic Engineering, IEEE, 31:850 – 861, 11 2006. doi: 10.1109/JOE.2006.886104.

J. Martínez. Processing chain for radar data. Technical Report 2, Servei d'Oceanografia Operacional, ICATMAR, 2023.

L. Quirós-Collazos, J. Ballabrera-Poy, C. Bueno, J. Martínez, S. Galiana, G. Llorach-Tó, C. González-Haro, G. Gantés, E. García-Ladona, and J. Isern-Fontanet. Estimating trajectories of floating objects using the new icatmar highfrequency radar network. Poster presented at the OceanPredict Symposium (OP'24) partnered with IOC-UNESCO,

Paris, France, 2024a. URL https://storageprdv2inwink.blob.core.windows.net/e2ed7ccb-dbb5-4dc9-9b30-9a6876d1fc19/d5541f76-555b-4b0d-b86e-d3d7989413ed.

L. Quirós-Collazos, C. Bueno-Herrero, J. Martínez, G. Llorach-Tó, C. González-Haro, J. Ribera-Altamir, J. Ballabrera, E. García-Ladona, and J. Isern-Fontanet. Level 3 velocity products from icatmar high-frequency radar network. Technical Report 3, Servei d'Oceanografia Operacional, ICATMAR, 2024b.

Philip L. Richardson. Eddy kinetic energy in the north atlantic from surface drifters. Journal of Geophysical Research: Oceans, 88(C7):4355–4367, 1983. doi: https://doi.org/10.1029/JC088iC07p04355.

R. Schmidt. Multiple emitter location and signal parameter estimation. IEEE Transactions on Antennas and Propagation, 34(3):276–280, 1986. doi: 10.1109/TAP.1986.1143830.

M. Smith, T. Updyke, and K. Wilcox. HFRadarPy (version 0.1.5.1), 2022. URL https://www.github.com/rucool/hfradarpy. (Accessed on 01/Feb/2023).

D.A. Trujillo, F.J. Kelly, J.C. Perez, H.R. Riddles, and J.S. Bonner. Accuracy of surface current velocity measurements obtained from hf radar in corpus christi bay, texas. In IGARSS 2004. 2004 IEEE International Geoscience and Remote Sensing Symposium, volume 2, pages 1179–1182, 2004. doi: 10.1109/IGARSS.2004.1368625.

US-IOOS. Manual for Real-Time Quality Control of High Frequency Radar Surface Current Data. US-IOOS, 2020.

Área de Medio Físico de Puertos del Estado. Red de boyas de aguas profundas. informe de datos de la boya de begur periodo: Dic.2021 - nov.2022. Technical report, Puertos del Estado, n.d.